

Astronomy 233 Spring 2011

Physical Cosmology

Week 2

General Relativity - Time and Distances

Joel Primack

University of California, Santa Cruz

General Relativity

GR follows from the principle of equivalence and Einstein's equation $G_{\mu\nu} \equiv R_{\mu\nu} - \frac{1}{2}Rg_{\mu\nu} = -8\pi GT_{\mu\nu}$.* Einstein had intuited the local equivalence of gravity and acceleration in 1907 ([Pais](#), p. 179), but it was not until November 1915 that he developed the final form of the GR equation.

(Gravitation & Cosmology)

It can be derived from the following assumptions ([Weinberg](#), p. 153):

1. The l.h.s. $G_{\mu\nu}$ is a tensor
2. $G_{\mu\nu}$ consists only of terms linear in second derivatives or quadratic in first derivatives of the metric tensor $g_{\mu\nu}$ ($\Leftrightarrow G_{\mu\nu}$ has dimension L^{-2})
3. Since $T_{\mu\nu}$ is symmetric in $\mu\nu$, so is $G_{\mu\nu}$
4. Since $T_{\mu\nu}$ is conserved (covariant derivative $T^{\mu}_{\nu;\mu}=0$) so also $G^{\mu}_{\nu;\mu}=0$
5. In the weak field limit where $g_{00} \approx -(1+2\phi)$, satisfying the Poisson equation $\nabla^2\phi=4\pi G\rho$ (i.e., $\nabla^2g_{00}=-8\pi GT_{00}$), we must have $G_{00}=\nabla^2g_{00}$

*Note: we're here using the metric $-1, 1, 1, 1$ as in [Dodelson](#), [Weinberg](#).

Einstein's equation can also be derived from an action principle, varying the total action $I = I_M + I_G$, where I_M is the action of matter and I_G is that of gravity:

$$I_G = - \frac{1}{16\pi G} \int R(x) \sqrt{g(x)} d^4x$$

(see, e.g., Weinberg, p. 364). The curvature scalar $R \equiv R_{\mu\nu} g^{\mu\nu}$ is the obvious term to insert in I_G since a scalar connected with the metric is needed and it is the only one, unless higher powers R^2 , R^3 or higher derivatives $\square R$ are used, which will lead to higher-order or higher-derivative terms in the gravity equation.

Einstein realized in 1916 that the 5th postulate above isn't strictly necessary – merely that the equation reduce to the Newtonian Poisson equation within observational errors, which allows the inclusion of a small cosmological constant term. In the action derivation, such a term arises if we just add a constant to R .

General Relativity: Observational Implications & Tests

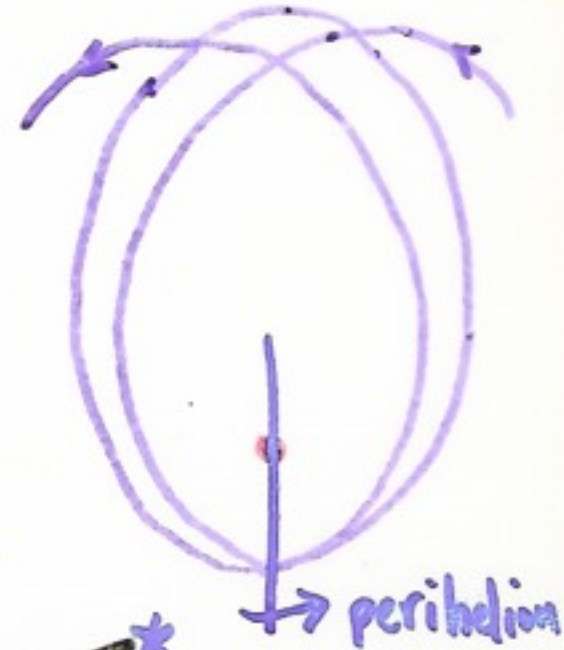
PERIHELION SHIFT OF ORBITS

finite speed of gravity, curvature

⇒ axis of elliptical orbit rotates

For Mercury, GR predicts $43''/\text{century}$

— just what Simon Newcomb saw!



DEFLECTION OF LIGHT

Newtonian & simple

equivalence principle prediction $\theta = 0.875''$

GR, including curvature ($\alpha + \beta + \gamma = 180^\circ - 0.875''$) ⇒ $\theta = 1.75''$

1919 Eddington eclipse expedition: $1.98 \pm 0.12''$

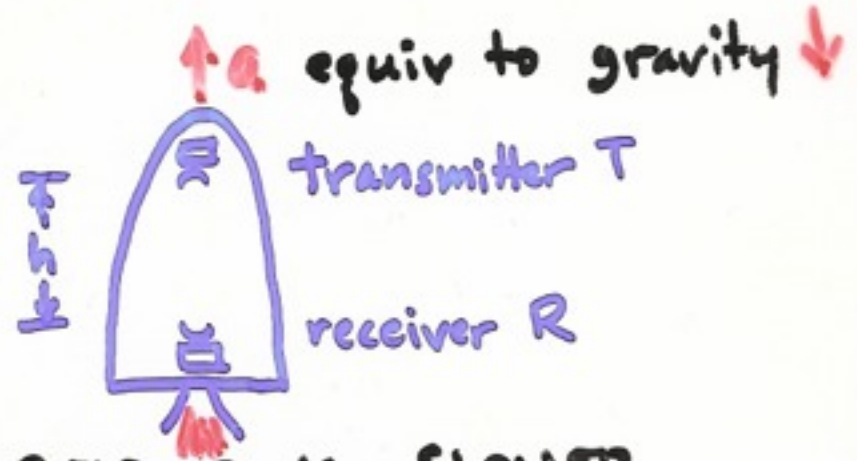


General Relativity: Observational Implications & Tests

GRAVITATIONAL REDSHIFT

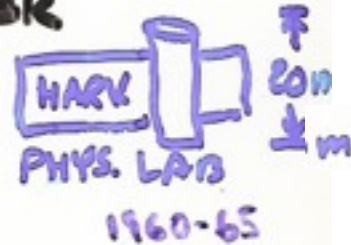
signals take $\Delta t = h/c$ from T \rightarrow R

R acquires $v = a \Delta t = a h/c$,
sees T's signal blueshifted



CLOCK IN STRONGER GRAV FIELD RUNS SLOWER

$$\text{fractional change} = \frac{a h}{c^2} = \frac{10 \frac{\text{m}}{\text{s}^2} 20 \text{ m}}{9 \times 10^{16} \text{ m}^2/\text{s}^2} = 2 \times 10^{-15}$$



Note that we are using Einstein's Principle of Equivalence:
locally, gravitation has exactly the same effect as acceleration
("strong" EEP version: this applies to all physical phenomena)

One elementary equivalence principle is the kind Newton had in mind when he stated that the property of a body called “mass” is proportional to the “weight”, and is known as the weak equivalence principle (WEP). An alternative statement of WEP is that the trajectory of a freely falling “test” body (one not acted upon by such forces as electromagnetism and too small to be affected by tidal gravitational forces) is independent of its internal structure and composition. In the simplest case of dropping two different bodies in a gravitational field, WEP states that the bodies fall with the same acceleration (this is often termed the Universality of Free Fall, or UFF).

The Einstein equivalence principle (EEP) is a more powerful and far-reaching concept; it states that:

1. WEP is valid.
2. The outcome of any local non-gravitational experiment is independent of the velocity of the freely-falling reference frame in which it is performed.
3. The outcome of any local non-gravitational experiment is independent of where and when in the universe it is performed.

The second piece of EEP is called local Lorentz invariance (LLI), and the third piece is called local position invariance (LPI).

For example, a measurement of the electric force between two charged bodies is a local non-gravitational experiment; a measurement of the gravitational force between two bodies (Cavendish experiment) is not.

The Einstein equivalence principle is the heart and soul of gravitational theory, for it is possible to argue convincingly that if EEP is valid, then gravitation must be a “curved spacetime” phenomenon, in other words, the effects of gravity must be equivalent to the effects of living in a curved spacetime. As a consequence of this argument, the only theories of gravity that can fully embody EEP are those that satisfy the postulates of “metric theories of gravity”, which are:

1. Spacetime is endowed with a symmetric metric.
2. The trajectories of freely falling test bodies are geodesics of that metric.
3. In local freely falling reference frames, the non-gravitational laws of physics are those written in the language of special relativity.

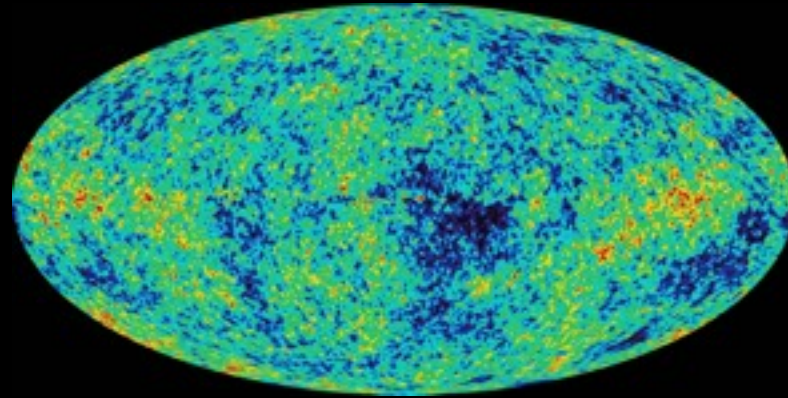
Renaissance of General Relativity 1960-

1960 QUASARS

1967 PULSARS

1974 BINARY PULSAR

1965 COSMIC BACKGROUND RADIATION



WMAP 2003

1971 BLACK HOLE CANDIDATES Cygnus X1...

1980 GRAVITATIONAL LENSES

Experimental Tests of General Relativity

	<u>Early</u>	<u>1960-70</u>	<u>1970-</u>	<u>Frontier</u>	
$m_{\text{inertial}} = m_{\text{gravitational}}$	Newton 10^{-3}	Eötvös 10^{-8}	Dicke 10^{-11}	Braginsky 10^{-12}	
Gravitational redshift		Pound 10^{-2}	airliner 10^{-1}	scout 10^{-4}	
Perihelion precession		Newcomb (43"/century) 10^{-2}	(Solar oblateness?)	binary pulsar (4°/yr)	Star-probe satellite
Light deflection		Eddington 10^{-1}	QSO: 10^{-2}	Grav. Lenses	
Time delay		Venus, Mercury 10^{-1}	Mars lander 10^{-3}		

Experimental Tests of General Relativity

Early

1960-70

1970-

frontier

Constancy
of G

Gravity
waves

Dragging of inertial
frames

Antimatter
falls up?

F vs. r ("5th force")

Mars lander
($|\dot{G}/G| < 10^{-11}/\text{yr}$)

binary pulsar
 $\sim 10^{-2}$

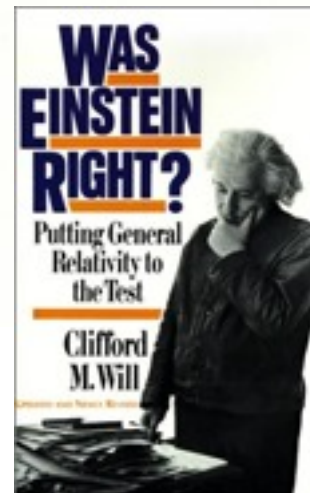
Antennas,
Lasers
(LIGO, LISA)

Gyro Satellite

Anti-proton
experiment

$1/r^2$ $r > \text{mm}$

see Clifford Will, *Was Einstein Right*
2nd Edition (Basic Books, 1993)



TESTS OF THE WEAK EQUIVALENCE PRINCIPLE

Clifford M. Will
“The Confrontation
Between General
Relativity and
Experiment”
*Living Reviews in
Relativity* (2001)

www.livingreviews.org

and his latest update
gr-qc/0510072

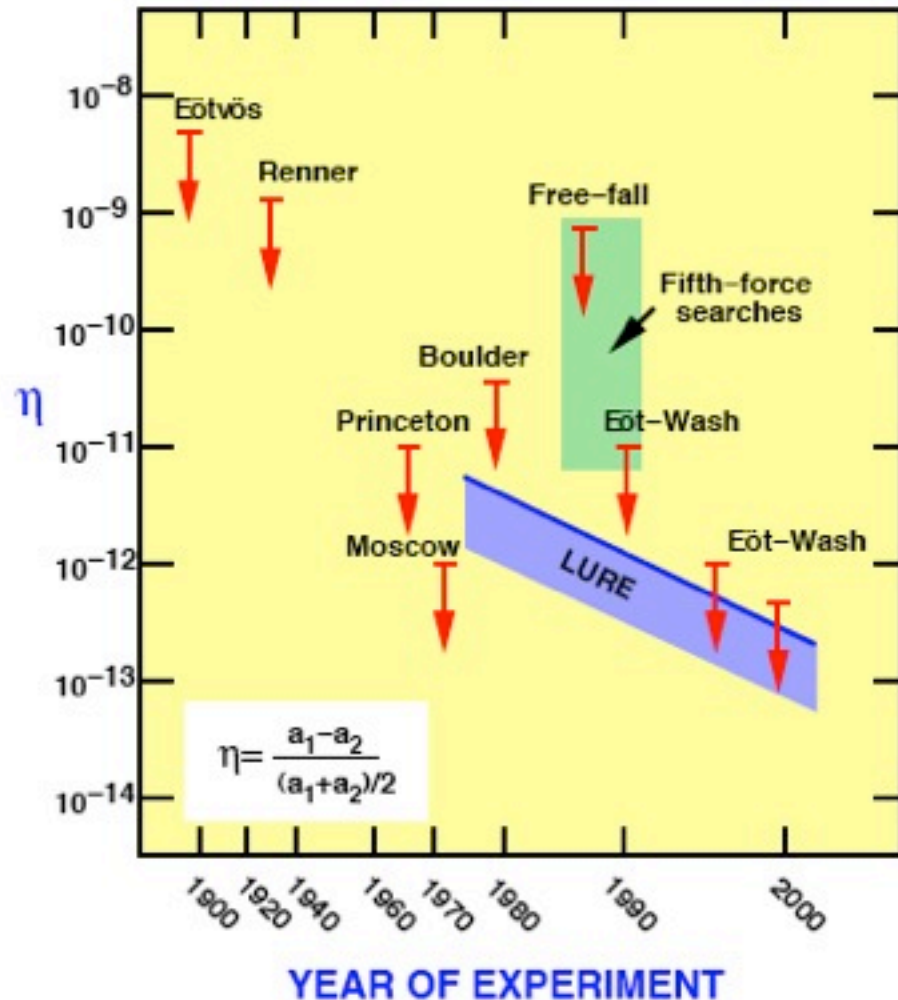


Figure 1: Selected tests of the weak equivalence principle, showing bounds on η , which measures fractional difference in acceleration of different materials or bodies. The free-fall and Eöt-Wash experiments were originally performed to search for a fifth force. The blue band shows current bounds on η for gravitating bodies from lunar laser ranging (LURE).

GRAVITATIONAL REDSHIFT TESTS

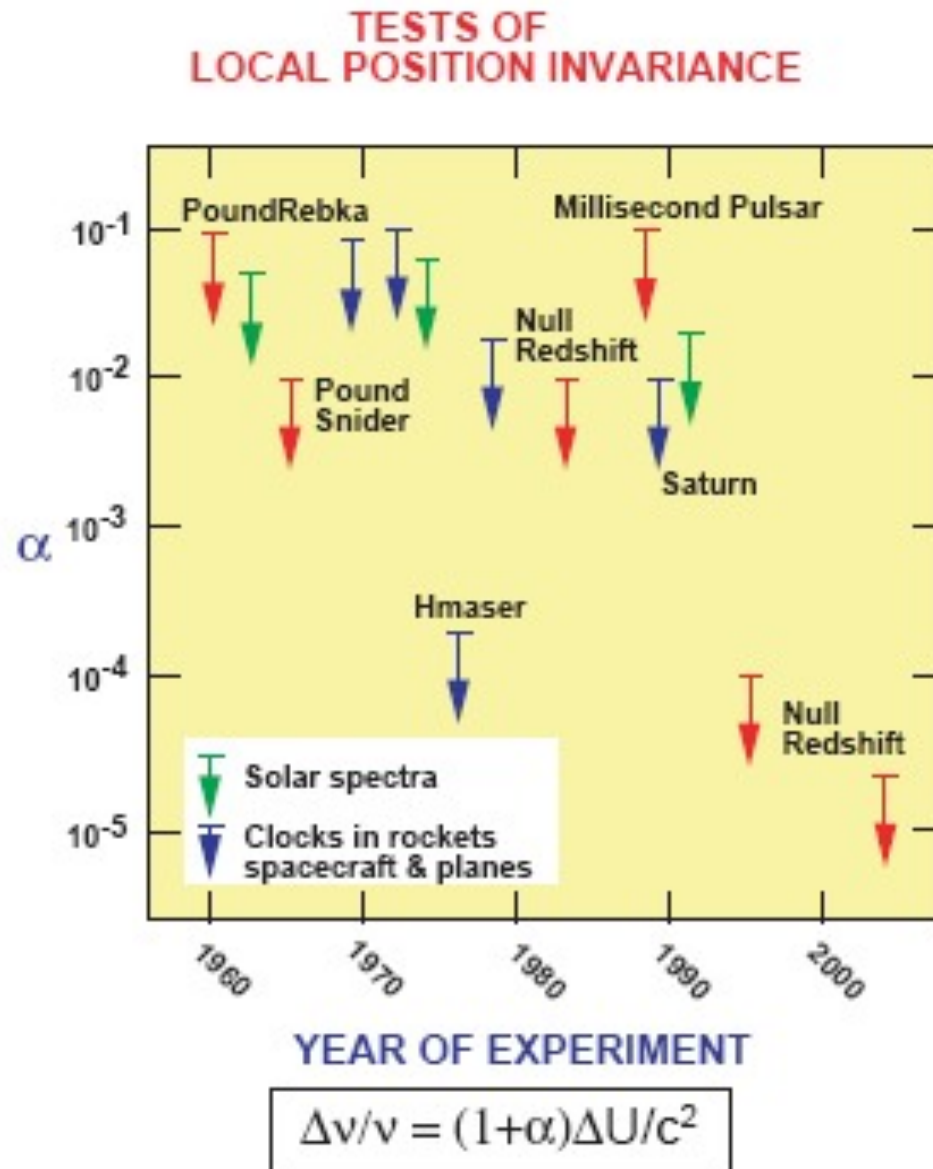
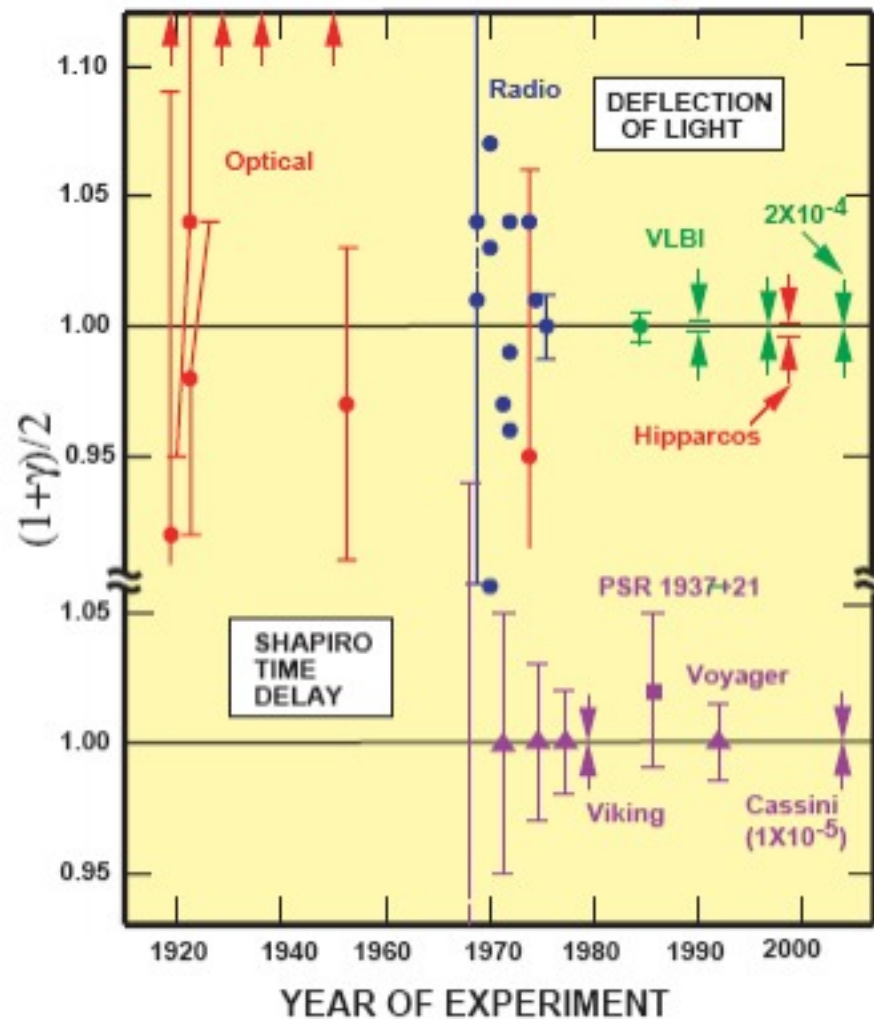


Figure 3: Selected tests of local position invariance via gravitational redshift experiments, showing bounds on α , which measures degree of deviation of redshift from the formula $\Delta\nu/\nu = \Delta U/c^2$.

Constancy of G



Method	$\dot{G}/G(10^{-13} \text{ yr}^{-1})$
Lunar Laser Ranging	4 ± 9
Binary Pulsar 1913 + 16	40 ± 50
Helioseismology	0 ± 16
Big Bang nucleosynthesis	0 ± 4

Figure 5: Measurements of the coefficient $(1 + \gamma)/2$ from light deflection and time delay measurements. Its GR value is unity. The arrows at the top denote anomalously large values from early eclipse expeditions. The Shapiro time-delay measurements using the Cassini spacecraft yielded an agreement with GR to 10^{-5} percent, and VLBI light deflection measurements have reached 0.02 percent. Hipparcos denotes the optical astrometry satellite, which reached 0.1 percent.

BINARY PULSAR

In 1993, the Nobel Prize in Physics was awarded to Russell Hulse and Joseph Taylor of Princeton University for their 1974 discovery of a pulsar, designated PSR1913+16, in orbit with another star around a common center of mass.

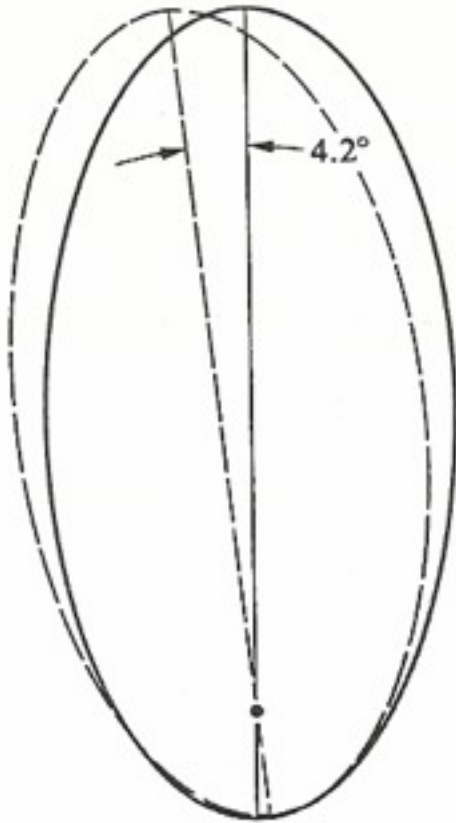


Figure 10.28. The rotation of the line of apsides in the binary pulsar amounts to 4.2 degrees per year. This effect has been interpreted to arise because the gravitational attraction of the companion deviates from a $1/r^2$ force law because of general-relativistic corrections.

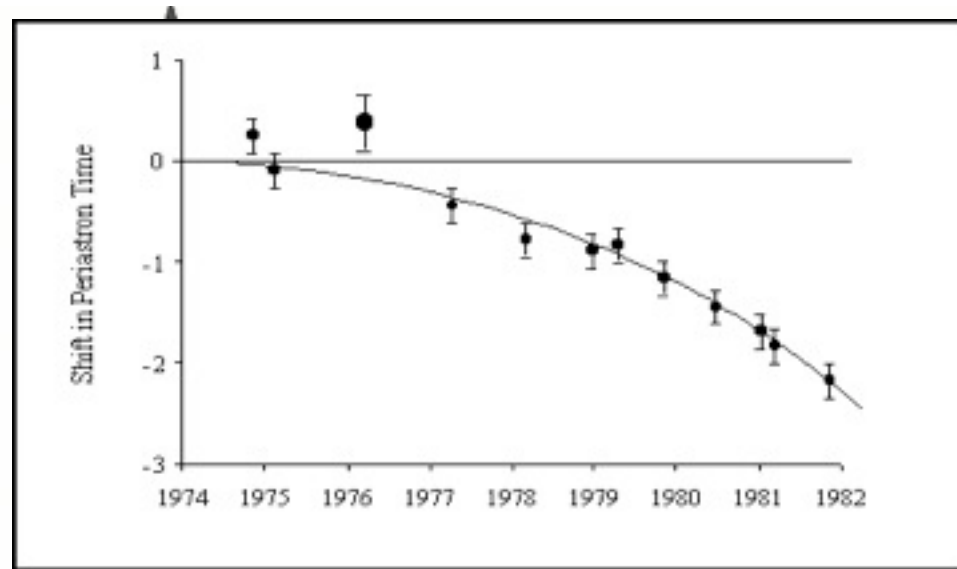


Figure 10.29. The decrease of the orbital period of the binary pulsar. This decrease is consistent with gravitational radiation causing a slow decay of the orbital separation as the two stars spiral slowly toward one another.

The pulsar is a rapidly rotating, highly magnetized neutron star which rotates on its axis 17 times per second. The pulsar is in a binary orbit with another star with a period of 7.75 hours.

BINARY PULSAR test of gravitational radiation

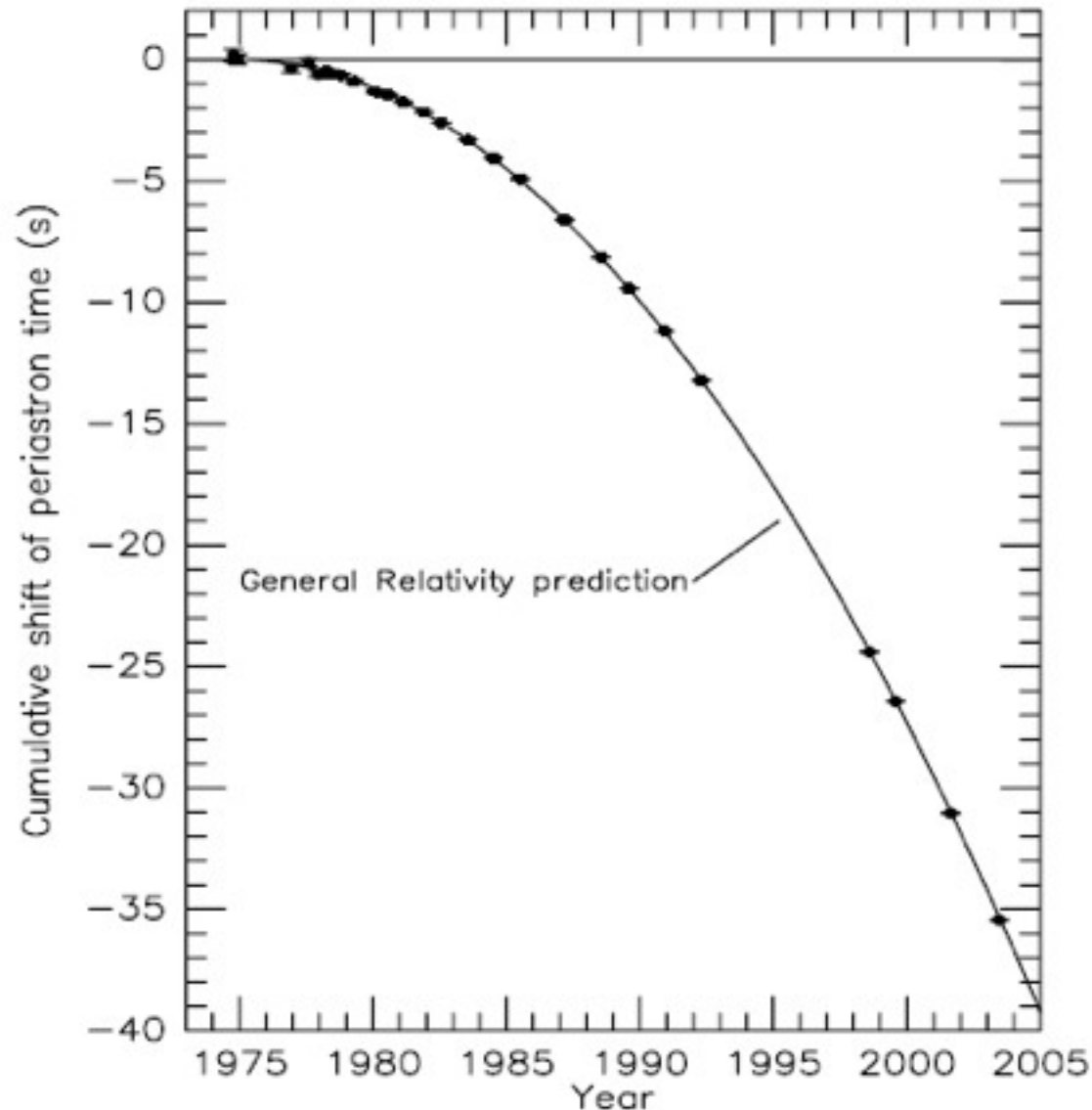
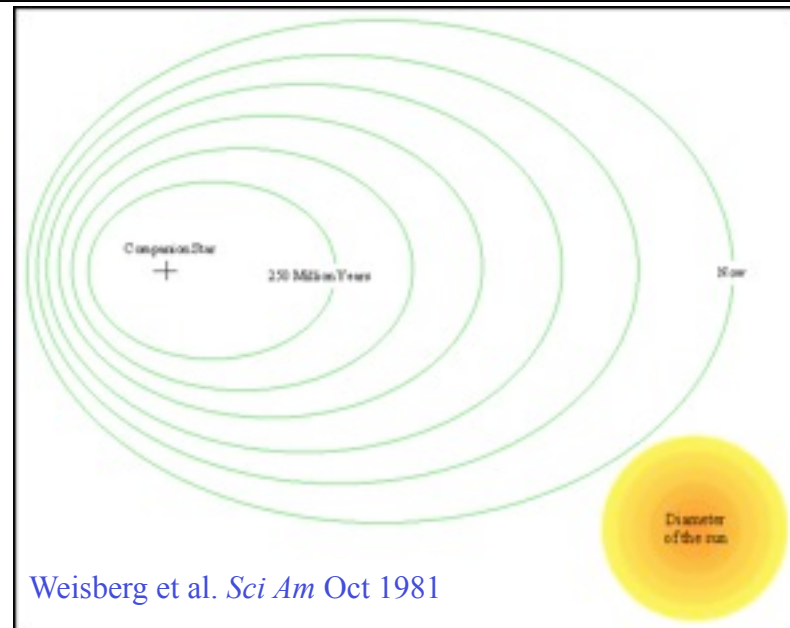
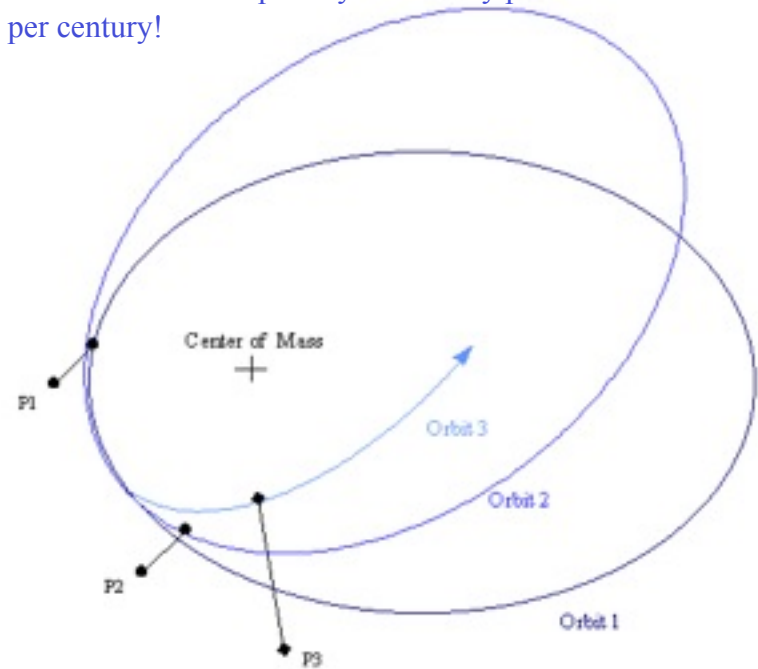


Figure 7: Plot of the cumulative shift of the periastron time from 1975–2005. The points are data, the curve is the GR prediction. The gap during the middle 1990s was caused by a closure of Arecibo for upgrading [243].

Data on the PSR B1913+16 system:

Right ascension	19h13m12.4655s
Declination	+16°01'08.189"
Distance	21,000 light years
Mass of detected pulsar	1.441 M_{Sun}
Mass of companion	1.387 M_{Sun}
Rotational period of detected pulsar	59.02999792988 sec
Diameter of each neutron star	20 km
Orbital period	7.751939106 hr
Eccentricity	0.617131
Semimajor axis	1,950,100 km
Periastron separation	746,600 km
Apastron separation	3,153,600 km
Orbital velocity of stars at periastron	300 km/sec
Orbital velocity of stars at apastron	75 km/sec
Rate of decrease of orbital period	0.0000765 sec per year
Rate of decrease of semimajor axis	3.5 meters per year
Calculated lifetime (to final inspiral)	300,000,000 years

Periastron advance per day = Mercury perihelion advance per century!



Weisberg et al. *Sci Am* Oct 1981

7 Conclusions

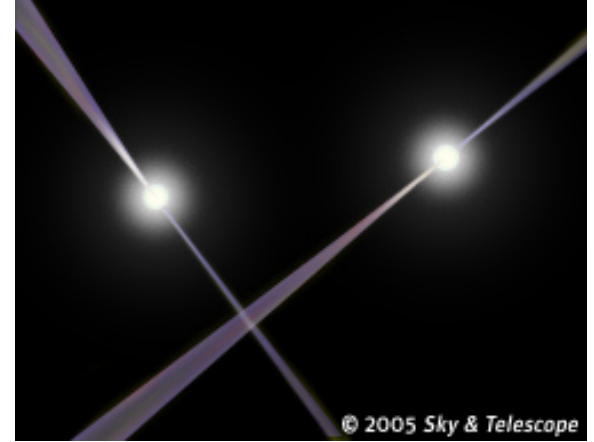
We find that general relativity has held up under extensive experimental scrutiny. The question then arises, why bother to continue to test it? One reason is that gravity is a fundamental interaction of nature, and as such requires the most solid empirical underpinning we can provide. Another is that all attempts to quantize gravity and to unify it with the other forces suggest that the standard general relativity of Einstein is not likely to be the last word. Furthermore, the predictions of general relativity are fixed; the theory contains no adjustable constants so nothing can be changed. Thus every test of the theory is either a potentially deadly test or a possible probe for new physics. Although it is remarkable that this theory, born 90 years ago out of almost pure thought, has managed to survive every test, the possibility of finding a discrepancy will continue to drive experiments for years to come.

Clifford Will, gr-qc/0510072

Einstein Passes New Tests

Sky & Telescope, March 3, 2005, by Robert Naeye

A binary pulsar system provides an excellent laboratory for testing some of the most bizarre predictions of general relativity. The two pulsars in the J0737-3039 system are actually very far apart compared to their sizes. In a true scale model, if the pulsars were the sizes of marbles, they would be about 750 feet (225 meters) apart.



Albert Einstein's 90-year-old general theory of relativity has just been put through a series of some of its most stringent tests yet, and it has passed each one with flying colors. Radio observations show that a recently discovered binary pulsar is behaving in lockstep accordance with Einstein's theory of gravity in at least four different ways, including the emission of gravitational waves and bizarre effects that occur when massive objects slow down the passage of time.

An international team led by Marta Burgay (University of Bologna, Italy) discovered the binary pulsar, known as J0737–3039 for its celestial coordinates, in late 2003 using the 64-meter Parkes radio telescope in Australia. Astronomers instantly recognized the importance of this system, because the two neutron stars are separated by only 800,000 kilometers (500,000 miles), which is only about twice the Earth–Moon distance. At that small distance, the two 1.3-solar-mass objects whirl around each other at a breakneck 300 kilometers per second (670,000 miles per hour), completing an orbit every 2.4 hours.

General relativity predicts that two stars orbiting so closely will throw off gravitational waves — ripples in the fabric of space-time generated by the motions of massive objects. By doing so, they will lose orbital energy and inch closer together. Radio observations from Australia, Germany, England, and the United States show that the system is doing exactly what Einstein's theory predicts. "The orbit shrinks by 7 millimeters per day, which is in accordance with general relativity," says Michael Kramer (University of Manchester, England), a member of the observing team.

A Review of The Double Pulsar - PSR J0737–3039

A. G. Lyne *

Table 1 Basic Observed Parameters of PSRs J0737–3039A and B

Pulsar	PSR J0737–3039A	PSR J0737–3039B
Pulse period P	22.7 ms	2.77 s
Period derivative \dot{P}	1.7×10^{-18}	0.88×10^{-15}
Orbital period P_b		2.45 hours
Eccentricity e		0.088
Orbital inclination		~ 88 deg
Projected semi-major axis x	1.42 sec	1.51 sec
Stellar mass M	$1.337(5) M_\odot$	$1.250(5) M_\odot$
Mean orbital velocity V_{orb}	301 km s^{-1}	323 km s^{-1}
Characteristic age τ	210 Myr	50 Myr
Magnetic field at surface B	$6.3 \times 10^9 \text{ G}$	$1.2 \times 10^{12} \text{ G}$
Radius of Light cylinder R_{LC}	1080 km	132 000 km
Spin-down luminosity \dot{E}	$6000 \times 10^{30} \text{ erg s}^{-1}$	$1.6 \times 10^{30} \text{ erg s}^{-1}$

2 TESTS OF GRAVITATIONAL THEORY

Non-relativistic binary systems are usually precisely described by the five Keplerian parameters, P_{orb} , $a \sin i$, e , ω and T_o and these are all accurately measured when one object is a pulsar. However, a number of general relativistic corrections to this classical description of the orbit - the so-called post-Keplerian (PK) parameters - are needed if the gravitational fields are sufficiently strong. In only a few months, using the Parkes Telescope, the Lovell Telescope at Jodrell Bank and the Green Bank Telescope, it was possible to measure several general relativistic effects in 6 months that took years to measure with the Hulse-Taylor binary pulsar, PSR B1913+16.

The following five PK relativistic parameters have already been measured in A, all causing small, but highly significant, modifications to the arrival times of the pulsars' radio pulses:

Relativistic periastron advance, $\dot{\omega}$. This is the rotation of the line connecting the two pulsars at their closest approach to one another. It arises from the distortion of space-time caused by the two stars, but can also be understood as the result of the finite time needed for the gravitational influence of one star to travel to another. This causes a time delay, during which the stars move so that the attractive force is no longer radial.

Gravitational redshift and time dilation, γ . The redshift results in clocks appearing to run slowly in a gravitational potential well and time dilation is the special relativistic effect which results in moving clocks appearing to run slowly. Both effects cause clocks close to a neutron star to tick more slowly than those further away. In other words the apparent pulse rate for A will slow down when it is close to B, and vice versa.

Shapiro delay, r and s . Radiation passing close to a massive body is delayed because its path length is increased by the curvature of space-time, an effect that Einstein overlooked but that was discovered in 1964 by Irwin Shapiro (Shapiro 1964) from radar measurements in the Solar System. Signals from A are measured after they have passed through the distorted space-time of B (in principle the effect could also be measured for the signals from B but its pulses are much broader and do not provide sufficient temporal resolution). The signal delay is essentially a function of two parameters: s , the shape, and r , the range, of the delay experienced by the pulses (with s being dependent on the inclination of the orbital plane and r on the mass of B).

Gravitational radiation and orbital decay, dP_b/dt . Almost every theory of gravitation predicts that the movement of massive bodies around one another in a binary system will result in the emission of gravitational waves. This emission causes the bodies to lose energy and hence to spiral into one another, so that they will eventually merge, creating a burst of gravitational waves when they do so. The rate of decrease of the orbital period, dP_b/dt , indicates that orbits of the pulsars are currently shrinking by about 7 mm per day.

5 CONCLUSION

Several fortunate circumstances have come together to make these studies possible. Not only is this a double-neutron-star system, but

- It has a very compact orbit, giving rise to intense gravitational fields and accelerations and hence abundant post-Keplerian gravitational effects
- One pulsar is a millisecond pulsar which enables these effects to be measured with high precision
- Both neutron stars are visible, allowing the mass-ratio to be determined
- Both pulsars have large flux densities, giving high-precision measurements
- The orbit is nearly edge on, so that the Shapiro delay can be measured with high precision.

All these properties enhance the quality and speed of the tests of gravitation theories in the strong-field regime. Furthermore, the last three also enable the investigations of the interactions between the stars and the probing of the magnetospheric properties.

Future observations of binary systems like PSR J0737–3039 promise to greatly increase our knowledge of strong-field gravity, but finding these systems will be a challenge. This is because double pulsars are extremely rare and, more importantly, because the Doppler effect causes their pulse periods to vary rapidly even during a short observation. It therefore becomes more difficult to detect the pulsars' periodicity using normal Fourier techniques and more sophisticated and computationally challenging search algorithms will have to be employed to uncover them.

Friedmann-Robertson-Walker Framework (homogeneous, isotropic universe)

$$\text{FRW } E(00) \quad \frac{\dot{a}^2}{a^2} = \frac{8\pi}{3}G\rho - \frac{k}{a^2} + \frac{\Lambda}{3} \quad \leftarrow \text{Friedmann equation}$$

$$\text{FRW } E(ii) \quad \frac{2\ddot{a}}{a} + \frac{\dot{a}^2}{a^2} = -8\pi Gp - \frac{k}{a^2} + \Lambda$$

$$H_0 \equiv 100h \text{ km s}^{-1} \text{ Mpc}^{-1} \\ \equiv 70h_{70} \text{ km s}^{-1} \text{ Mpc}^{-1}$$

$$\frac{E(00)}{H_0^2} \Rightarrow 1 = \Omega_0 - \frac{k}{H_0^2 a^2} + \Omega_\Lambda \text{ with } H \equiv \frac{\dot{a}}{a}, a_0 \equiv 1, \Omega_0 \equiv \frac{\rho_0}{\rho_c}, \Omega_\Lambda \equiv \frac{\Lambda}{3H_0^2}, \\ \rho_{c,0} \equiv \frac{3H_0^2}{8\pi G} = 1.36 \times 10^{11} h_{70}^2 M_\odot \text{ Mpc}^{-3}$$

$$E(ii) - E(00) \Rightarrow \frac{2\ddot{a}}{a} = -\frac{8\pi}{3}G\rho - 8\pi Gp + \frac{2}{3}\Lambda$$

$$\text{Divide by } 2E(00) \Rightarrow q_0 \equiv -\left(\frac{\ddot{a}}{a} \frac{a^2}{\dot{a}^2}\right)_0 = \frac{\Omega_0}{2} - \Omega_\Lambda$$

$$E(00) \Rightarrow t_0 = \int_0^1 \frac{da}{a} \left[\frac{8\pi}{3}G\rho - \frac{k}{a^2} + \frac{\Lambda}{3} \right]^{-\frac{1}{2}} = H_0^{-1} \int_0^1 \frac{da}{a} \left[\frac{\Omega_0}{a^3} - \frac{k}{H_0^2 a^2} + \Omega_\Lambda \right]^{-\frac{1}{2}}$$

$$t_0 = H_0^{-1} f(\Omega_0, \Omega_\Lambda) \quad H_0^{-1} = 9.78 h^{-1} \text{ Gyr} \quad f(1, 0) = \frac{2}{3} \\ = 13.97 h_{70}^{-1} \text{ Gyr} \quad f(0, 0) = 1 \\ f(0, 1) = \infty \\ f(0.3, 0.7) = 0.964$$

$$[E(00)a^3]' \text{ vs. } E(ii) \Rightarrow \frac{\partial}{\partial a}(\rho a^3) = -3p a^2 \text{ ("continuity")}$$

Given eq. of state $p = p(\rho)$, integrate to determine $\rho(a)$,
integrate $E(00)$ to determine $a(t)$

$$\text{Matter: } p = 0 \Rightarrow \rho = \rho_0 a^{-3} \text{ (assumed above in } q_0, t_0 \text{ eqs.)}$$

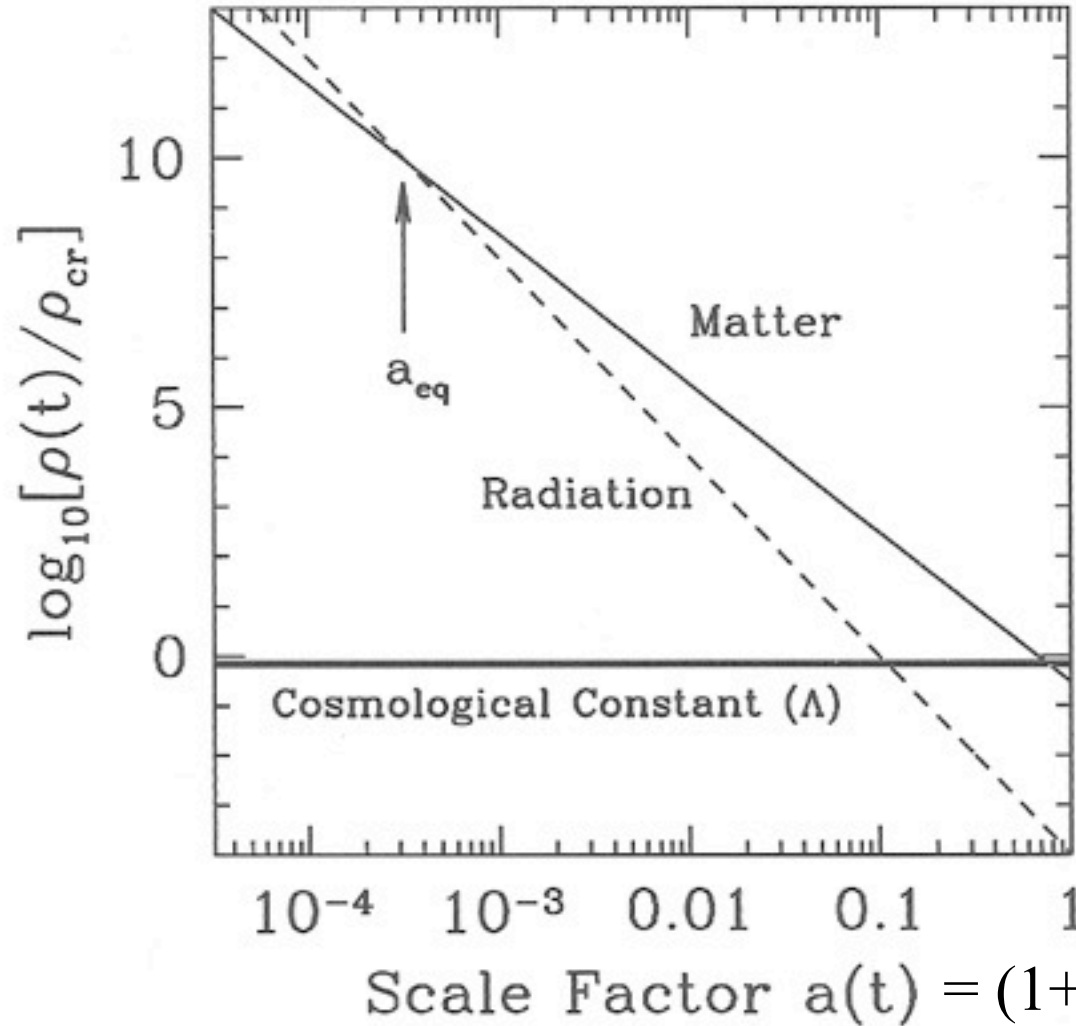
$$\text{Radiation: } p = \frac{\rho}{3}, k = 0 \Rightarrow \rho \propto a^{-4}$$

LCDM Benchmark Cosmological Model: Ingredients & Epochs

	List of Ingredients
photons:	$\Omega_{\gamma,0} = 5.0 \times 10^{-5}$
neutrinos:	$\Omega_{\nu,0} = 3.4 \times 10^{-5}$
total radiation:	$\Omega_{r,0} = 8.4 \times 10^{-5}$
baryonic matter:	$\Omega_{\text{bary},0} = 0.04$
nonbaryonic dark matter:	$\Omega_{\text{dm},0} = 0.26$
total matter:	$\Omega_{m,0} = 0.30$
cosmological constant:	$\Omega_{\Lambda,0} \approx 0.70$

	Important Epochs	
radiation-matter equality:	$a_{rm} = 2.8 \times 10^{-4}$	$t_{rm} = 4.7 \times 10^4 \text{ yr}$
matter-lambda equality:	$a_{m\Lambda} = 0.75$	$t_{m\Lambda} = 9.8 \text{ Gyr}$
Now:	$a_0 = 1$	$t_0 = 13.5 \text{ Gyr}$

Evolution of Densities of Radiation, Matter, & Λ



$z = \text{redshift}$

Figure 1.3. Energy density vs scale factor for different constituents of a flat universe. Shown are nonrelativistic matter, radiation, and a cosmological constant. All are in units of the critical density today. Even though matter and cosmological constant dominate today, at early times, the radiation density was largest. The epoch at which matter and radiation are equal is a_{eq} .

Dodelson,
Chapter 1

Benchmark Model: Scale Factor vs. Time

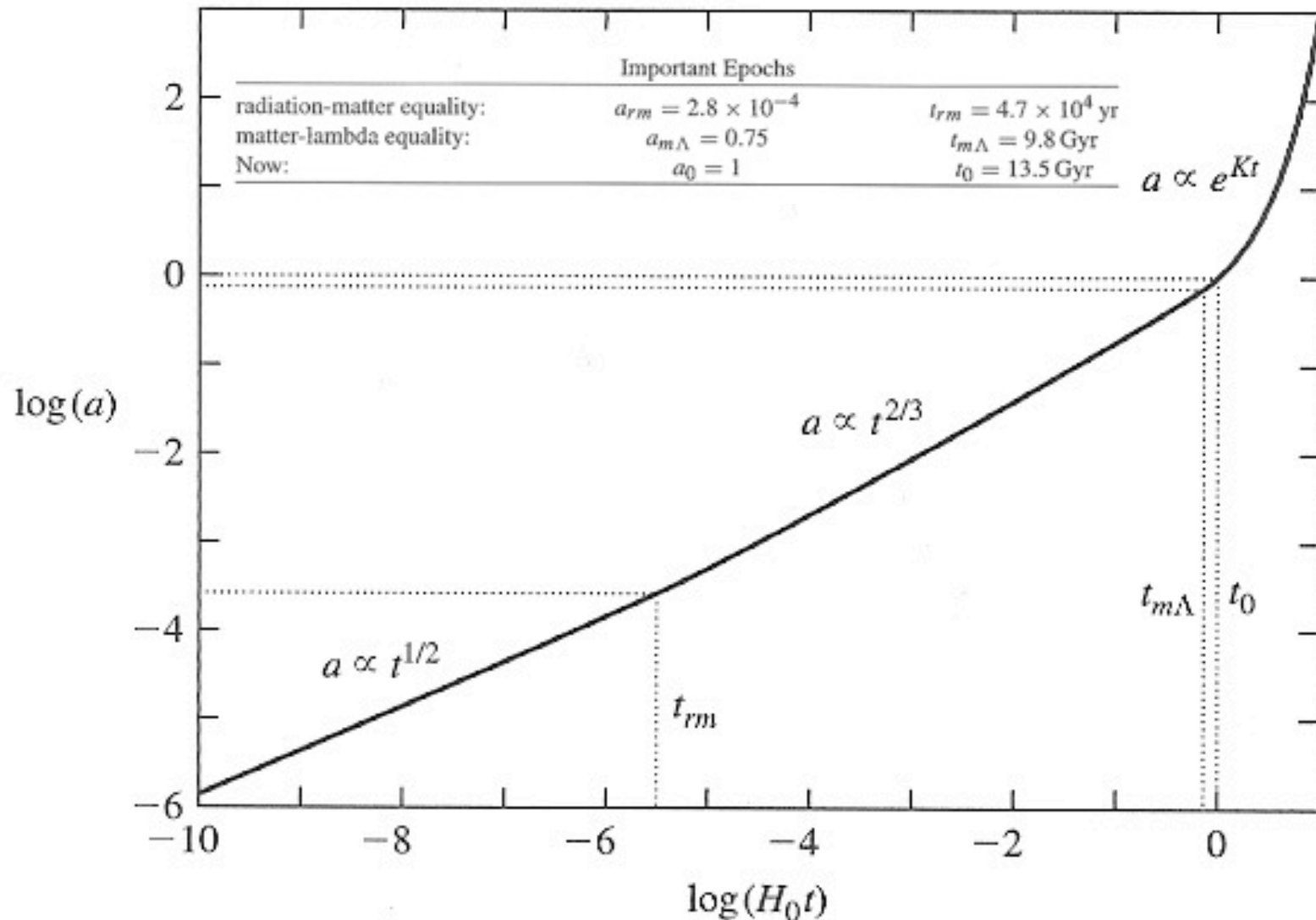
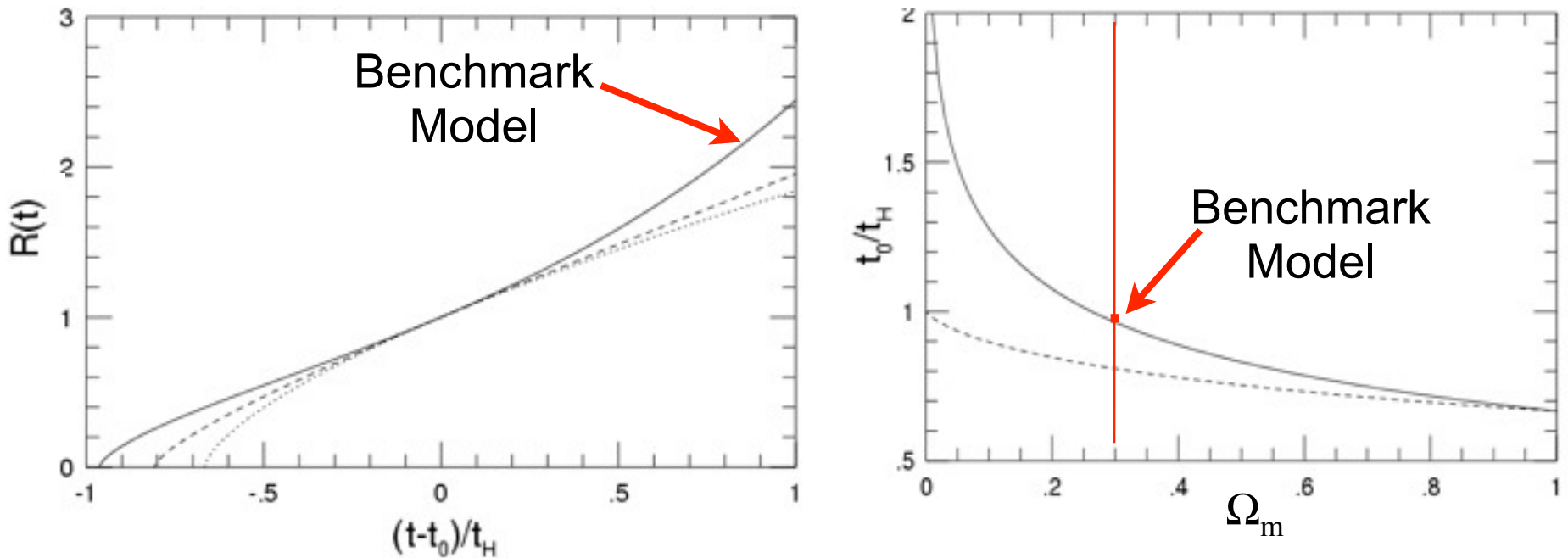


FIGURE 6.5 The scale factor a as a function of time t (measured in units of the Hubble time), computed for the Benchmark Model. The dotted lines indicate the time of radiation-matter equality, $a_{rm} = 2.8 \times 10^{-4}$, the time of matter-lambda equality, $a_{m\Lambda} = 0.75$, and the present moment, $a_0 = 1$.

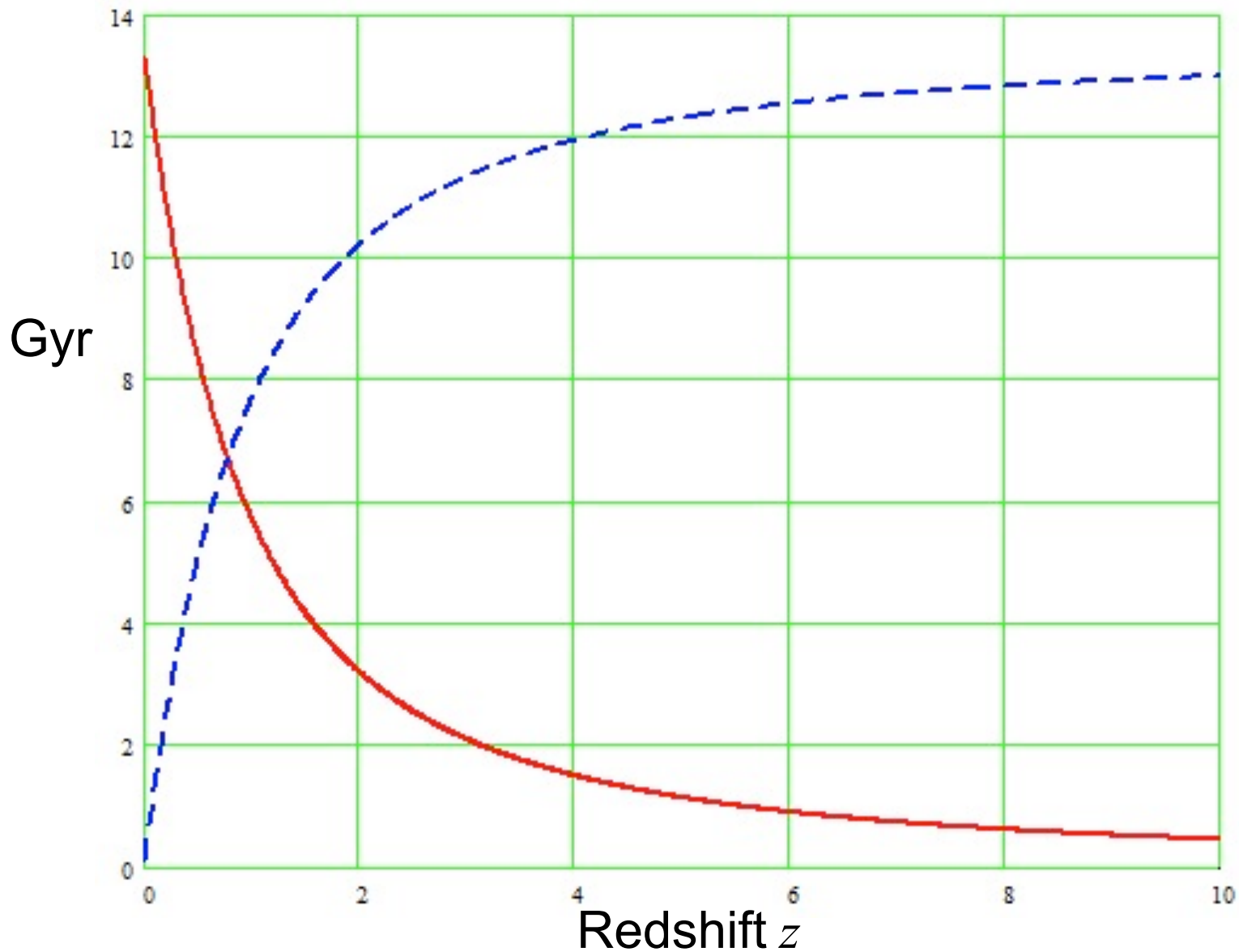
Barbara Ryden, *Introduction to Cosmology* (Addison-Wesley, 2003)

Age of the Universe t_0 in FRW Cosmologies



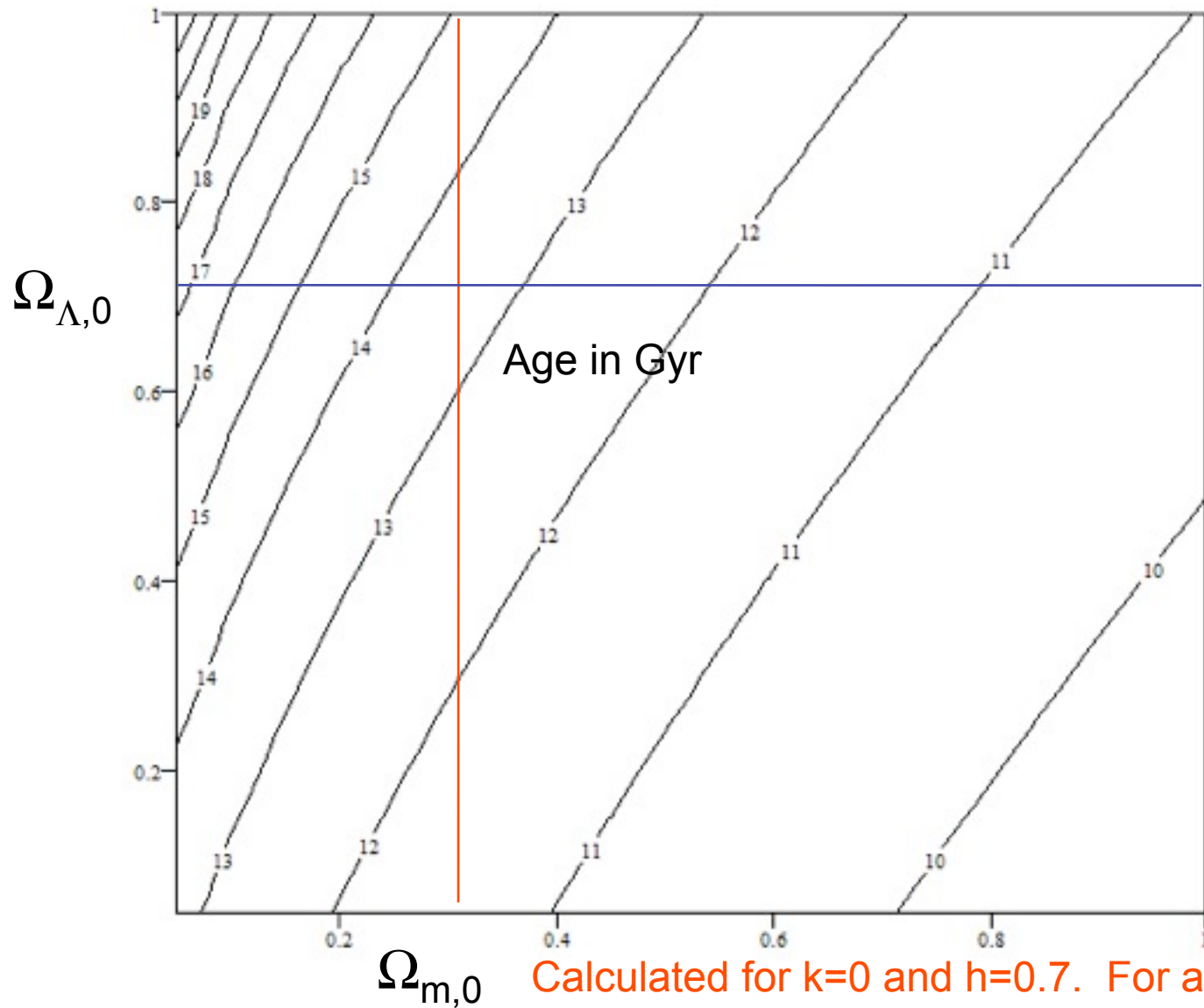
(a) Evolution of the scale factor $a(t)$ plotted vs. the time after the present $(t - t_0)$ in units of Hubble time $t_H \equiv H_0^{-1} = 9.78h^{-1}$ Gyr for three different cosmologies: Einstein-de Sitter ($\Omega_0 = 1, \Omega_\Lambda = 0$ dotted curve), negative curvature ($\Omega_0 = 0.3, \Omega_\Lambda = 0$: dashed curve), and low- Ω_0 flat ($\Omega_0 = 0.3, \Omega_\Lambda = 0.7$: solid curve). (b) Age of the universe today t_0 in units of Hubble time t_H as a function of Ω_0 for $\Lambda = 0$ (dashed curve) and flat $\Omega_0 + \Omega_\Lambda = 1$ (solid curve) cosmologies.

Age of the Universe and Lookback Time



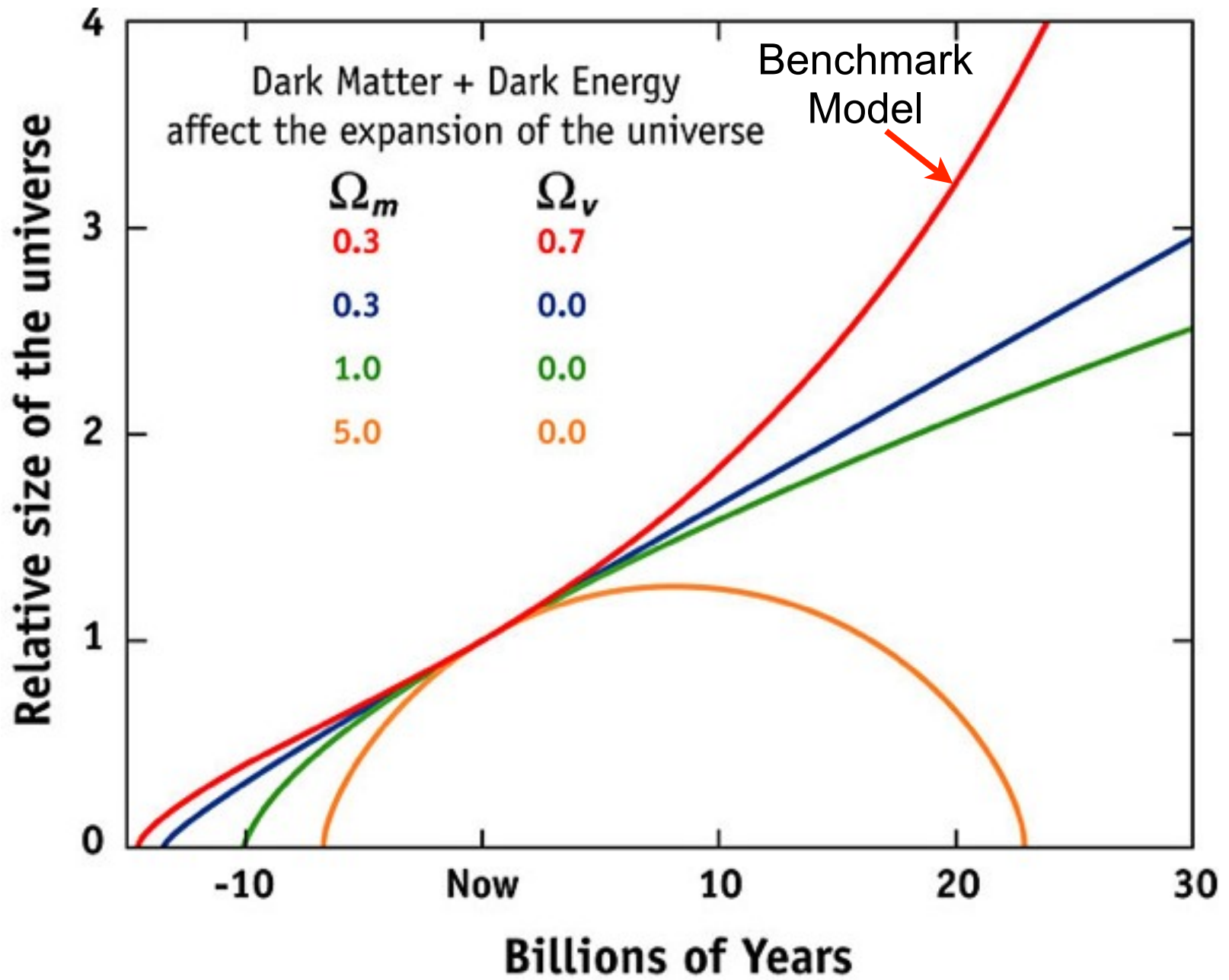
These are for the **Benchmark Model** $\Omega_{m,0}=0.3$, $\Omega_{\Lambda,0}=0.7$, $h=0.7$.

Age t_0 of the Double Dark Universe



Calculated for $k=0$ and $h=0.7$. For any other value of the Hubble parameter, multiply the age by $(h/0.7)$.

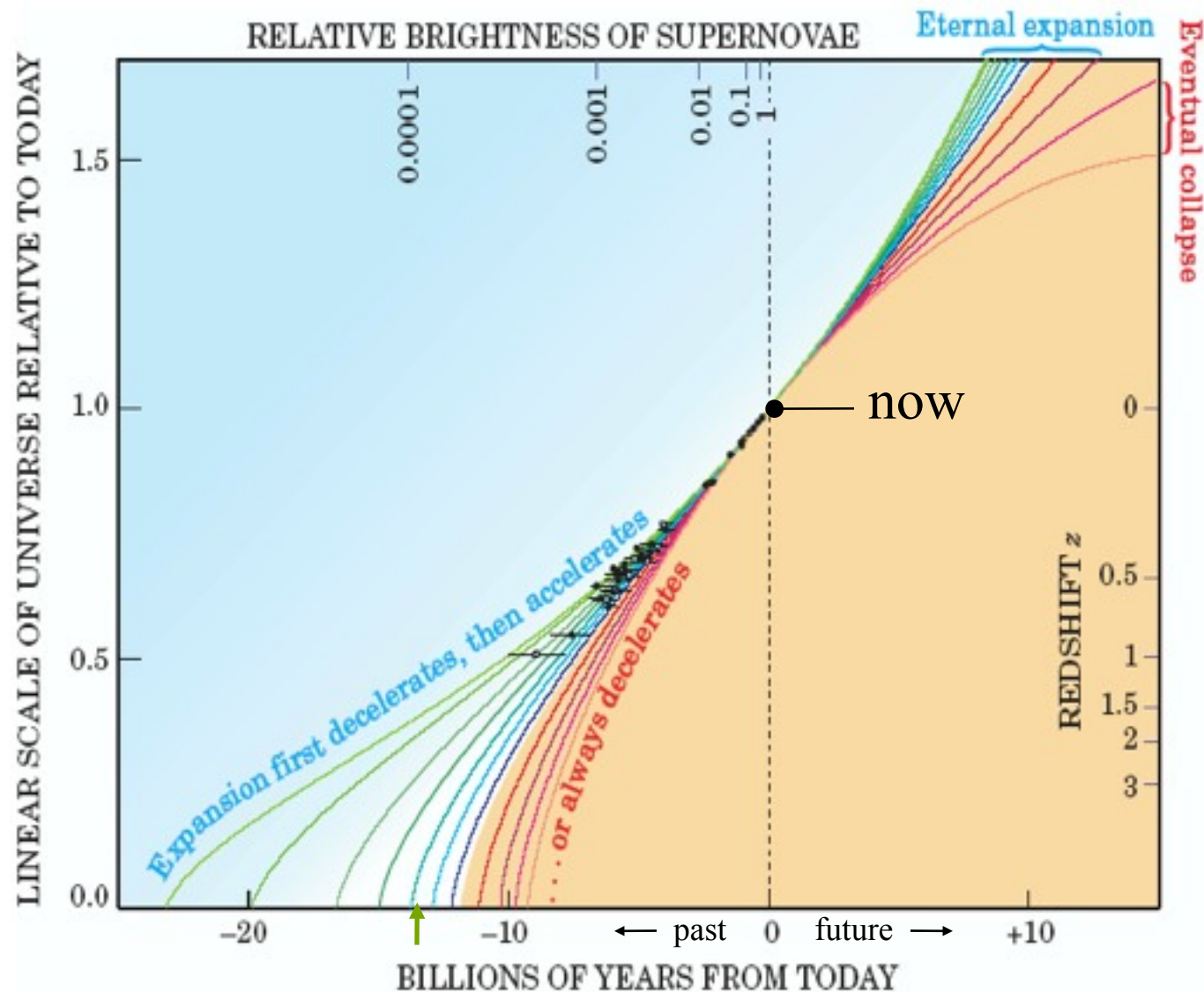
History of Cosmic Expansion for General Ω_M & Ω_Λ

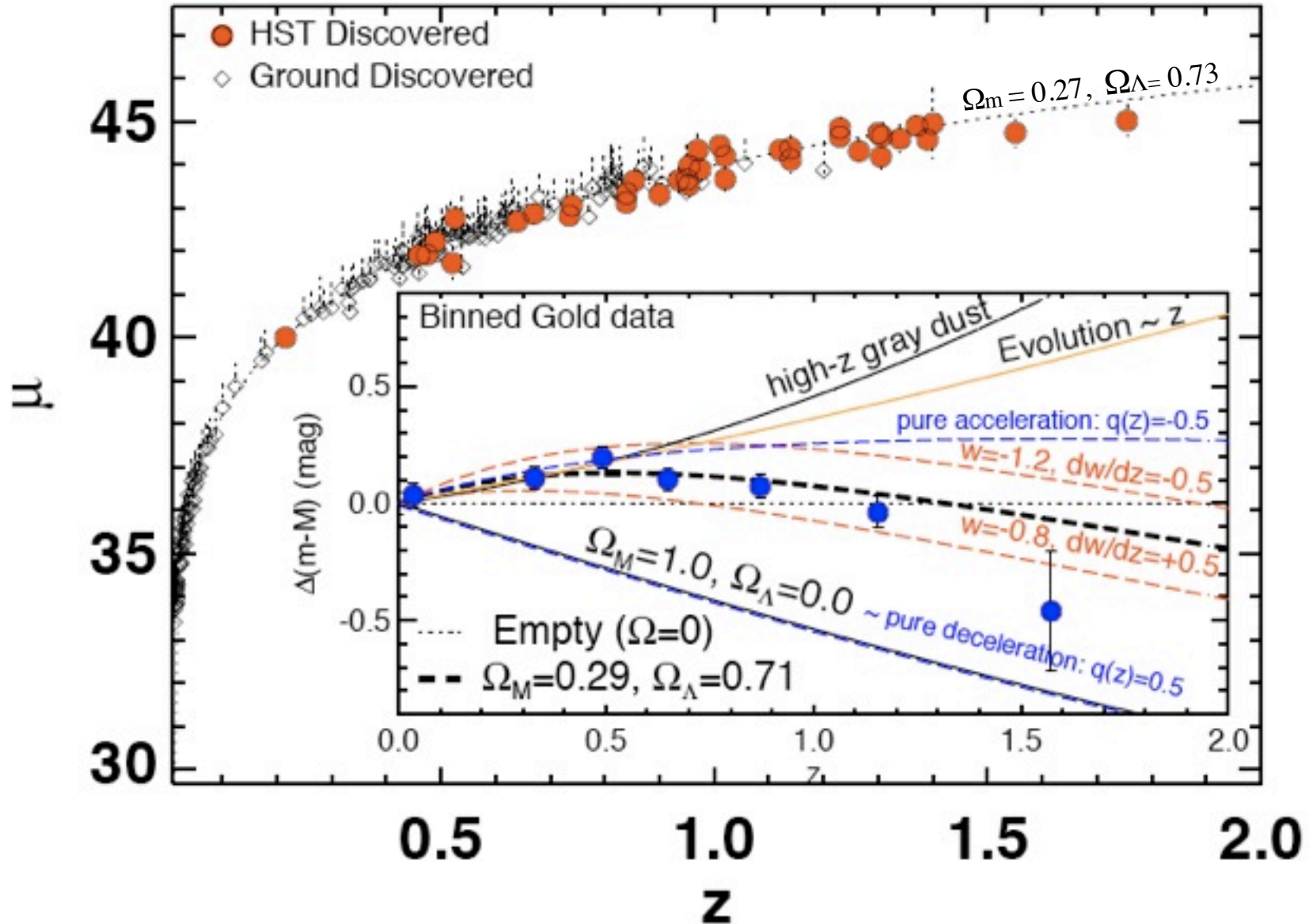


History of Cosmic Expansion for $\Omega_\Lambda = 1 - \Omega_M$

With $\Omega_\Lambda = 0$ the age of the decelerating universe would be only 9 Gyr, but $\Omega_\Lambda = 0.7, \Omega_M = 0.3$ gives an age of 14 Gyr, consistent with stellar and radioactive decay ages

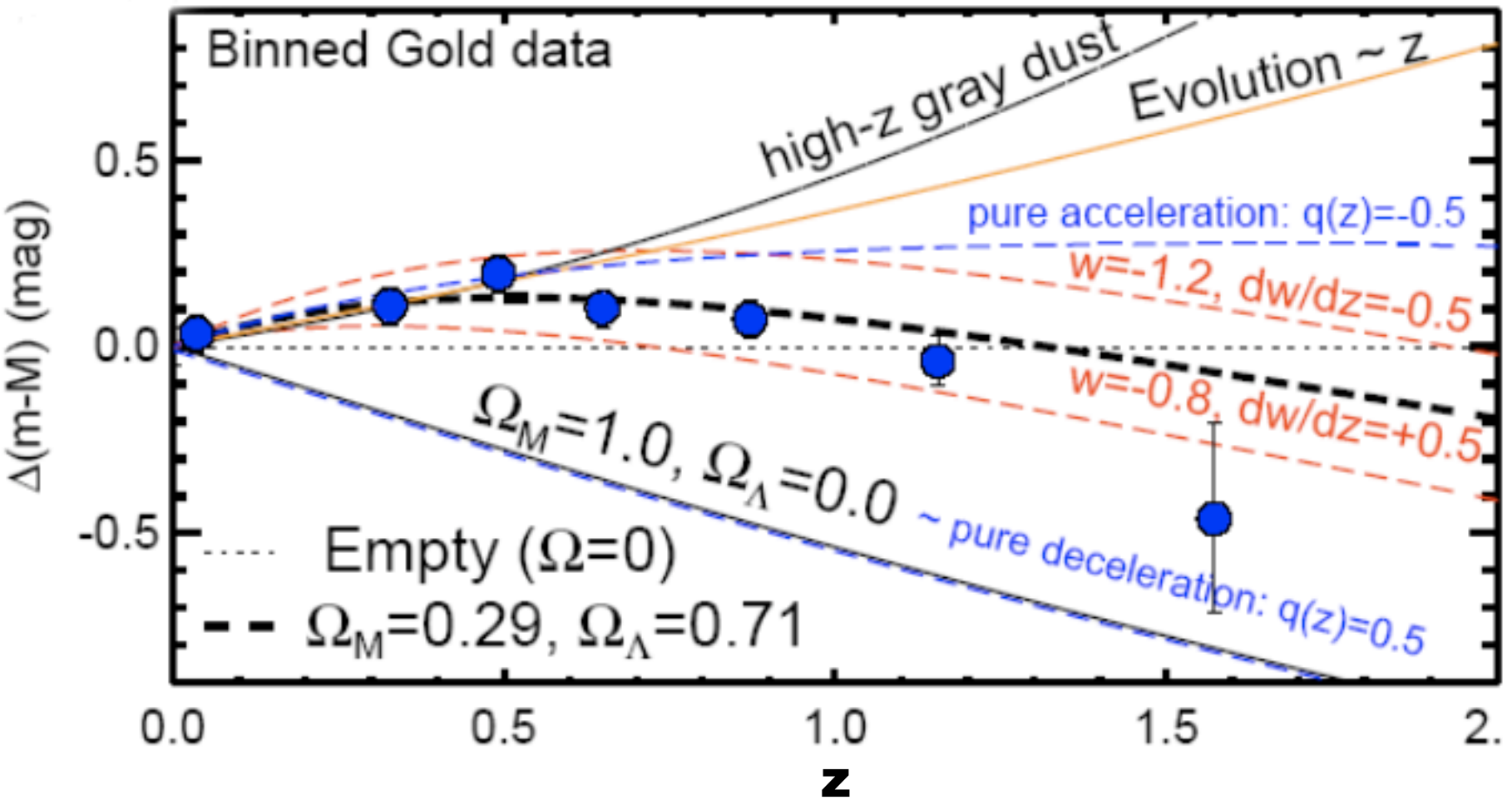
Figure 4. The history of cosmic expansion, as measured by the high-redshift supernovae (the black data points), assuming flat cosmic geometry. The scale factor R of the universe is taken to be 1 at present, so it equals $1/(1+z)$. The curves in the blue shaded region represent cosmological models in which the accelerating effect of vacuum energy eventually overcomes the decelerating effect of the mass density. These curves assume vacuum energy densities ranging from $0.95 \rho_c$ (top curve) down to $0.4 \rho_c$. In the yellow shaded region, the curves represent models in which the cosmic expansion is always decelerating due to high mass density. They assume mass densities ranging (left to right) from $0.8 \rho_c$ up to $1.4 \rho_c$. In fact, for the last two curves, the expansion eventually halts and reverses into a cosmic collapse.



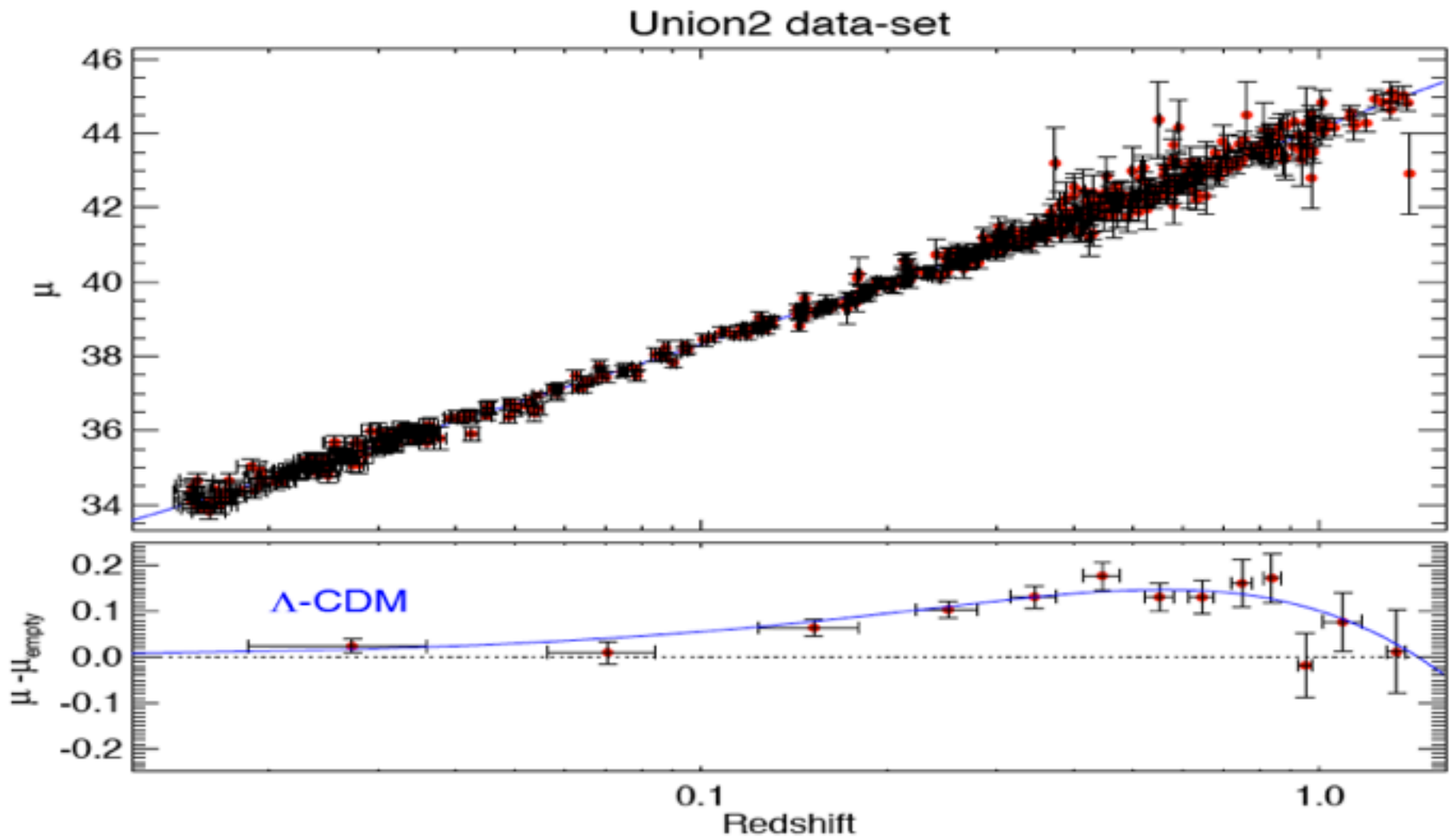


SNe Ia from ground-based discoveries in the Gold sample are shown as diamonds, HST-discovered SNe Ia are shown as filled symbols. Overplotted is the best fit for a flat cosmology: $\Omega_m = 0.27$, $\Omega_\Lambda = 0.73$.

Inset: Residual Hubble diagram and models after subtracting empty Universe model. The Gold sample is binned in equal spans of $n\Delta z = 6$ where n is the number of SNe in a bin and z is the redshift range of the bin. Fig. 6 of A. Riess et al. 2007, ApJ, 659, 98.



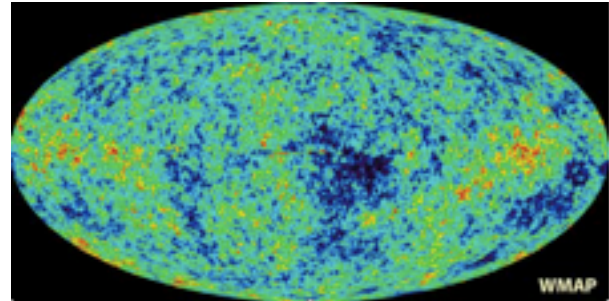
From the [A. Riess et al. 2007, ApJ, 659, 98 Abstract](#): The unique leverage of the HST high-redshift SNe Ia provides the first meaningful constraint on the dark energy equation-of-state parameter at $z \geq 1$. The result remains consistent with a cosmological constant ($w(z) = -1$), and rules out rapidly evolving dark energy ($dw/dz \gg 1$). The defining property of dark energy, its negative pressure, appears to be present at $z > 1$, in the epoch preceding acceleration, with $\sim 98\%$ confidence in our primary fit. Moreover, the $z > 1$ sample-averaged spectral energy distribution is consistent with that of the typical SN Ia over the last 10 Gyr, indicating that any spectral evolution of the properties of SNe Ia with redshift is still below our detection threshold.



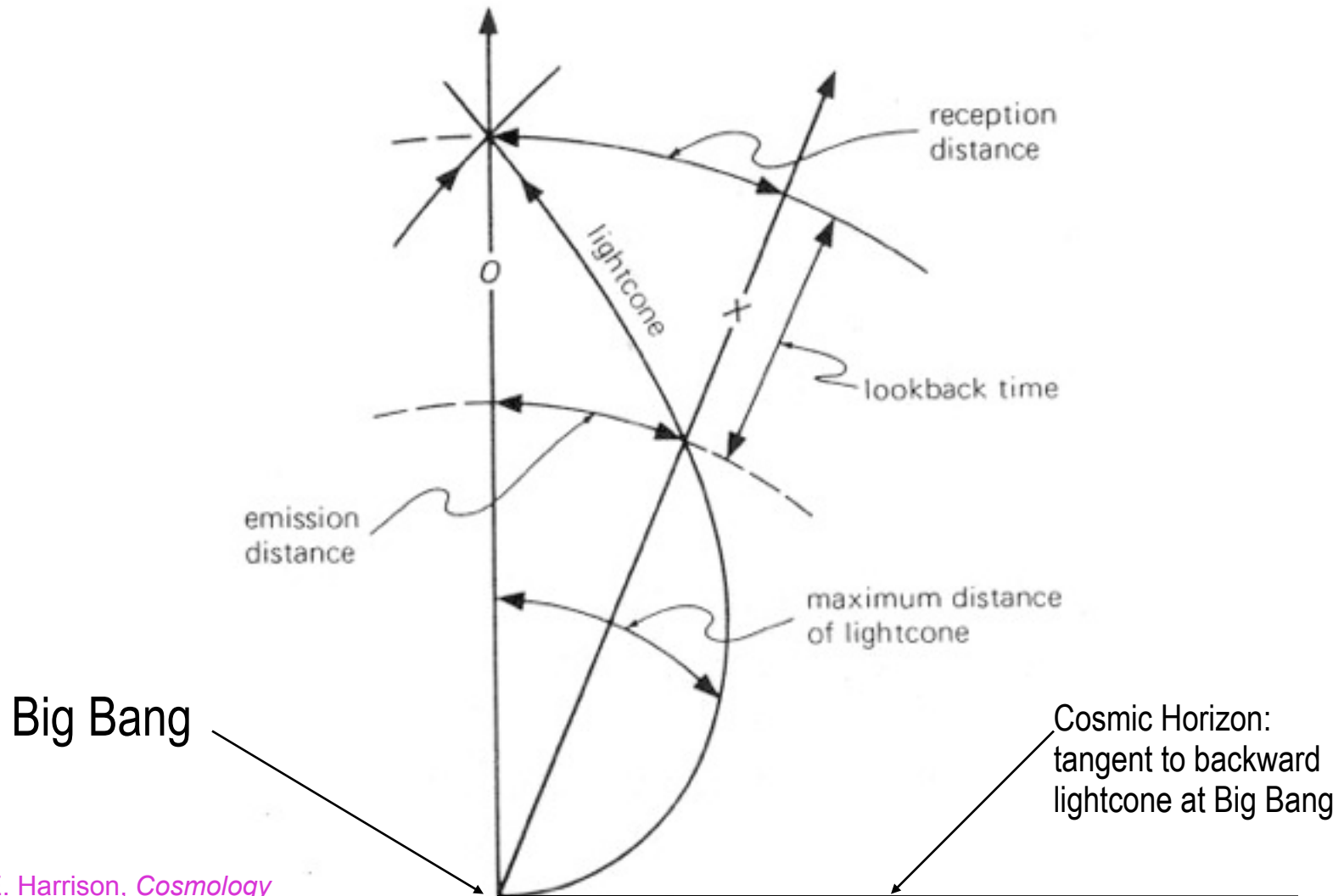
The Hubble diagram of Type Ia supernovae correlating distance modulus (μ) vs. redshift. The Union2 compilation (Amanullah R, Lidman C, Rubin D, Aldering G, Astier P, et al., 2010) represents the currently largest SN Ia sample. The linear expansion in the local universe can be traced out to $z < 0.1$. The distance relative to an empty universe model (μ_{empty}) is shown in the lower panel. The data are binned for clarity in this diagram. The blue curve shows the expectation from the best fit Λ CDM model with $\Omega_m = 0.3$.

Brief History of the Universe

- Cosmic Inflation generates density fluctuations
- Symmetry breaking: more matter than antimatter
- All antimatter annihilates with almost all the matter (1s)
- Big Bang Nucleosynthesis makes light nuclei (10 min)
- Electrons and light nuclei combine to form atoms, and the cosmic background radiation fills the newly transparent universe (380,000 yr)
- Galaxies and larger structures form (~ 1 Gyr)
- Carbon, oxygen, iron, ... are made in stars
- Earth-like planets form around 2nd generation stars
- Life somehow starts (~ 4 Gyr ago) and evolves on earth



Picturing the History of the Universe: The Backward Lightcone



From E. Harrison, *Cosmology*
(Cambridge UP, 2000).

Picturing the History of the Universe: The Backward Lightcone

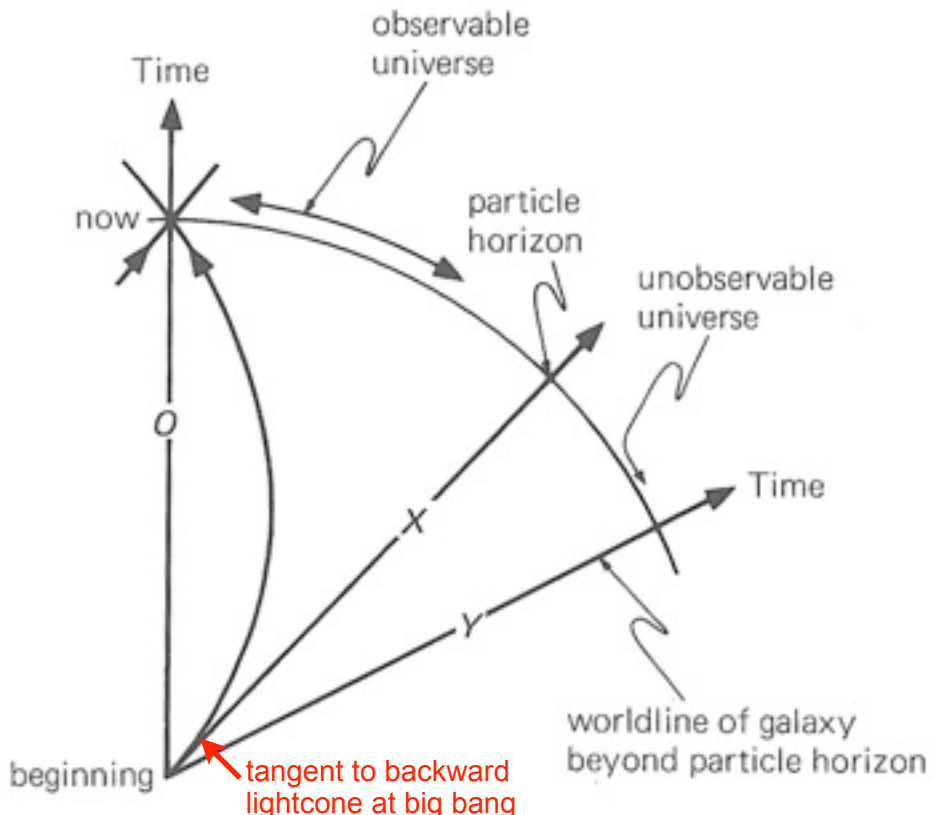


Figure 21.11. At the instant labeled "now" the particle horizon is at worldline X. In a big bang universe, all galaxies at the particle horizon have infinite redshift.

From E. Harrison, *Cosmology* (Cambridge UP, 2000).

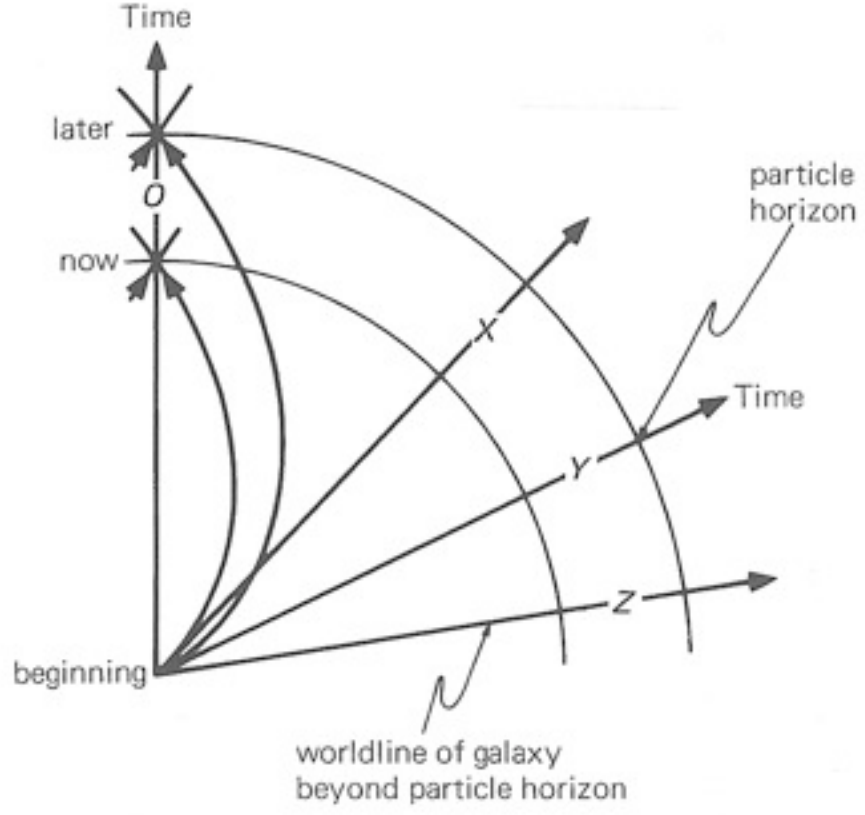


Figure 21.12. At the instant labeled "later" the particle horizon has receded to world line Y. Notice the distance of the particle horizon is always a reception distance, and the particle horizon always overtakes the galaxies and always the fraction of the universe observed increases.

Distances in an Expanding Universe

Proper distance = physical distance = d_p

$$d_p(t_0) = (\text{physical distance at } t_0) = a(t_0) r_e = r_e$$

$\chi(t_e) =$ (comoving distance of galaxy emitting at time t_e)

$$\chi(t_e) = \int_0^{r_e} dr = r_e = c \int_{t_e}^{t_0} dt/a = c \int_{a_e}^1 da/(a^2 H)$$

because

$$dt = (dt/da) da = (a dt/da) da/a = da/(aH)$$

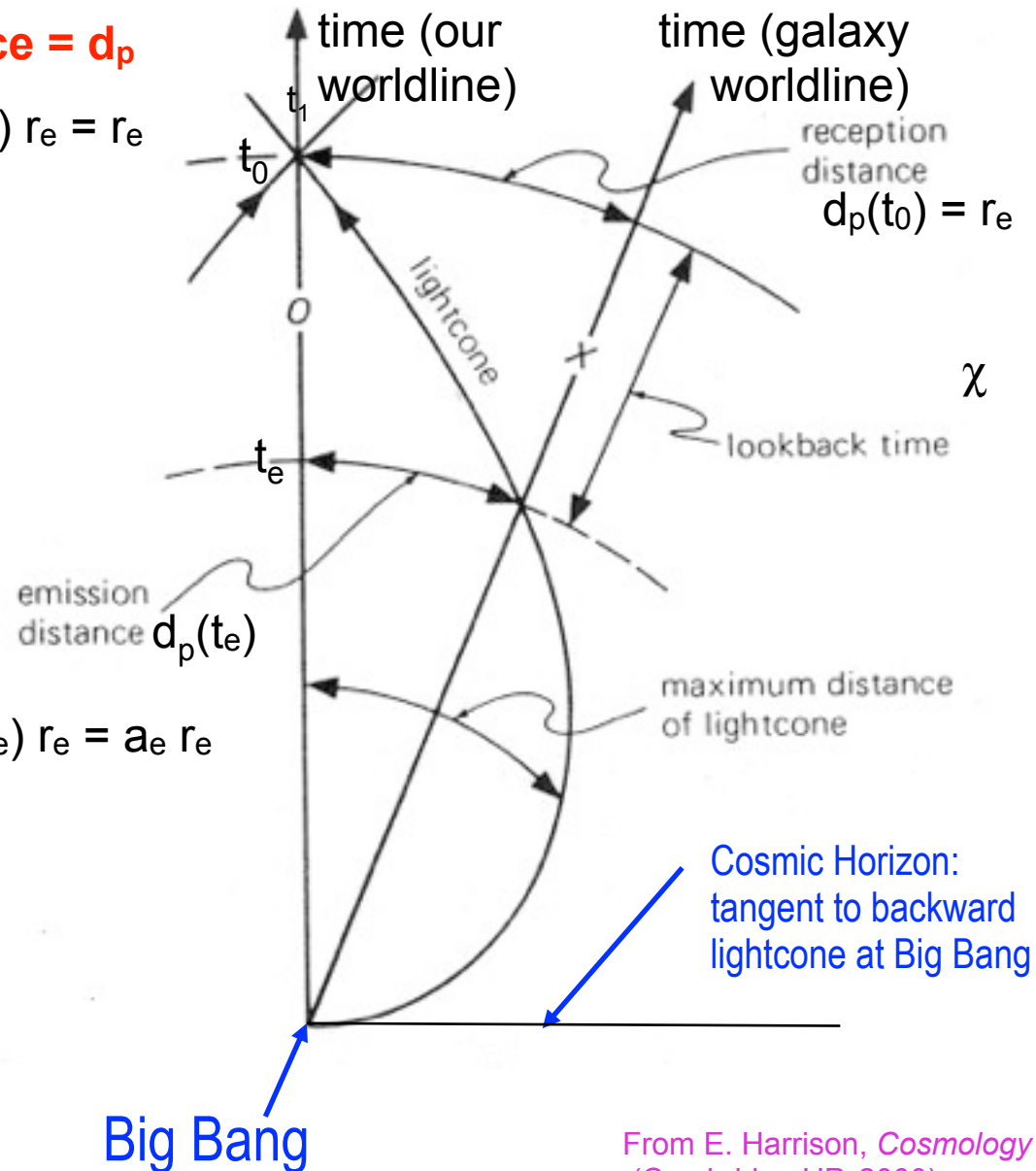
$$d_p(t_e) = (\text{physical distance at } t_e) = a(t_e) r_e = a_e r_e$$

The Hubble radius $d_H = c H_0^{-1} =$
 $= 4.29 h_{70}^{-1} \text{ Gpc} = 13.97 h_{70}^{-1} \text{ Glyr}$

For E-dS, where $H = H_0 a^{-3/2}$,

$$\chi(t_e) = r_e = d_p(t_0) = 2d_H (1 - a_e^{1/2})$$

$$d_p(t_e) = 2d_H a_e (1 - a_e^{1/2})$$



From E. Harrison, *Cosmology* (Cambridge UP, 2000).

Horizons

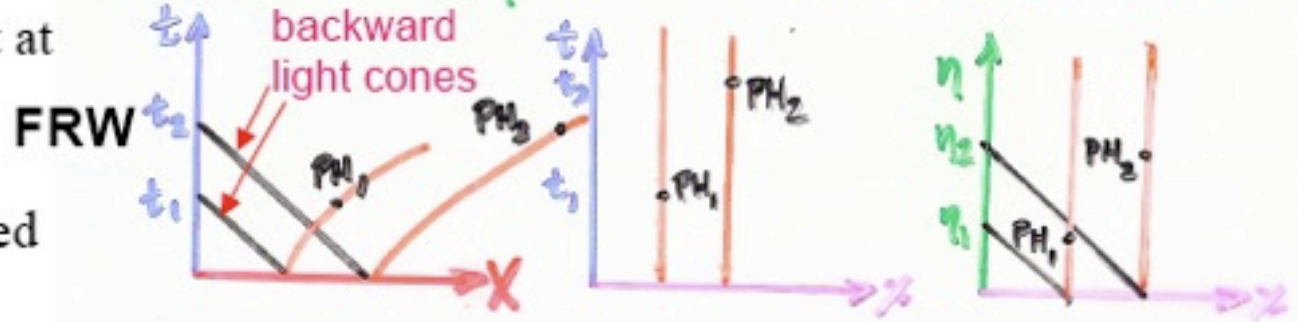
PARTICLE HORIZON

Spherical surface that at time t separates *worldlines* into observed vs. unobserved

$$ds^2 = dt^2 - dX^2 = dt^2 - R^2 dz^2 = R^2 (d\eta^2 - dx^2)$$

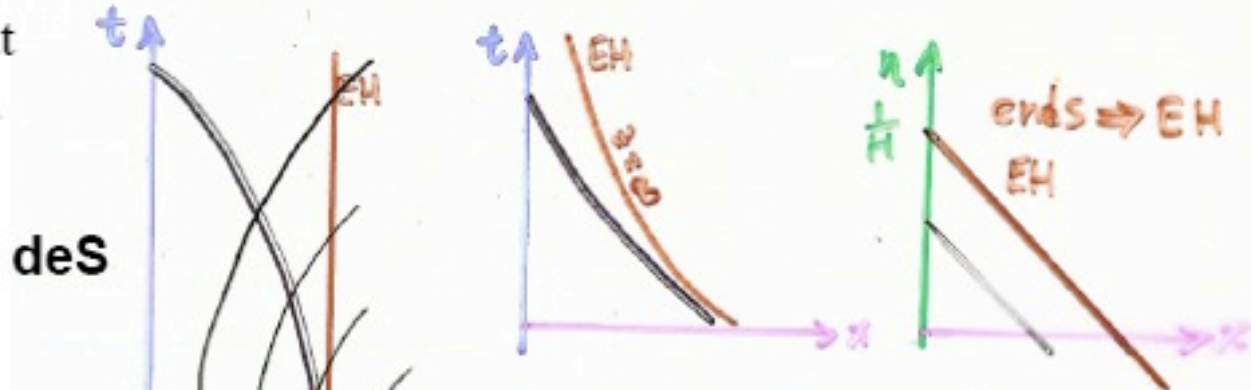
conformal time $d\eta = dt/R$

comoving coord. $dx = dX/R$



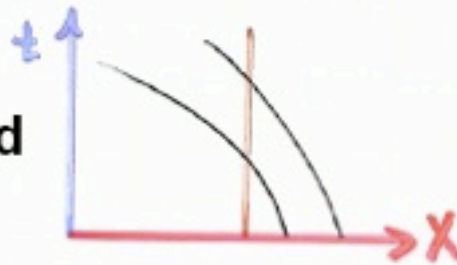
EVENT HORIZON

Backward lightcone that separates *events* that will someday be observed from those never observed



$$\eta = \int_{t_0}^{\infty} \frac{dt}{e^{Ht}} = \frac{1}{H} e^{-Ht_0} \leq \frac{1}{H}$$

Schwarzschild



See Harrison, *Cosmology*
Rindler, *Relativity*

Distances in an Expanding Universe

FRW: $ds^2 = -c^2 dt^2 + a(t)^2 [dr^2 + r^2 d\theta^2 + r^2 \sin^2\theta d\phi^2]$ for curvature $k=0$

$$\chi(t_1) = (\text{comoving distance at time } t_1) = \int_0^{t_1} dt/a = r_1$$

$$d(t_1) = (\text{physical distance at } t_1) = a(t_1) \chi(t_1)$$

Particle $\chi_p = (\text{comoving distance at time } t_0) = r_p$

Horizon $d_p = (\text{physical distance at time } t_0) = a(t_0) r_p = r_p$
 since $a(t_0) = 1$

From the FRW metric above, the distance D across a source at distance r_1 which subtends an angle $d\theta$ is $D = a(t_1) r_1 d\theta$. The angular diameter distance d_A is defined by $d_A = D/d\theta$, so

$$d_A = a(t_1) r_1 = r_1 / (1+z_1)$$

In Euclidean space, the luminosity L of a source at distance d is related to the apparent luminosity ℓ by

$$\ell = \text{Power/Area} = L/4\pi d^2$$

so the luminosity distance d_L is defined by $d_L = (L/4\pi\ell)^{1/2}$.

Weinberg, *Cosmology*, pp. 31-32, shows that in FRW

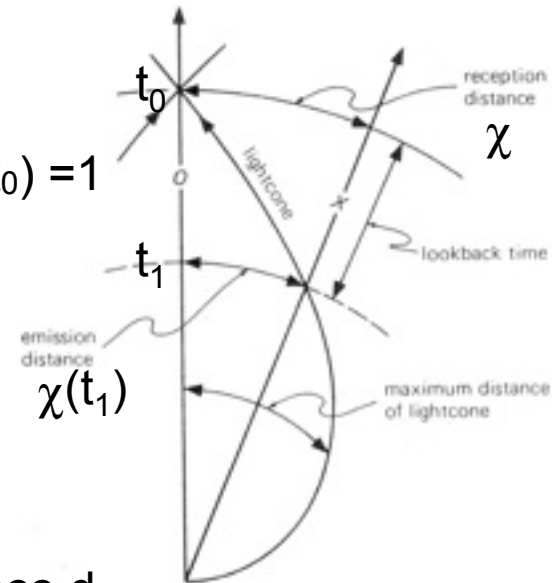
$$\ell = \text{Power/Area} = L [a(t_1)/a(t_0)]^2 [4\pi a(t_0)^2 r_1^2]^{-1} = L/4\pi d_L^2$$

Thus

$$d_L = r_1/a(t_1) = r_1 (1+z_1)$$

fraction of photons reaching unit area at t_0
 (redshift of each photon)(delay in arrival)

adding distances at time t_1



Distances in a Flat ($k=0$) Expanding Universe

$$\chi(t_1) = (\text{comoving distance at time } t_1) = r_1 \quad d_A = a(t_1) r_1 = r_1/(1+z_1) \quad d_L = r_1/a(t_1) = r_1 (1+z_1)$$

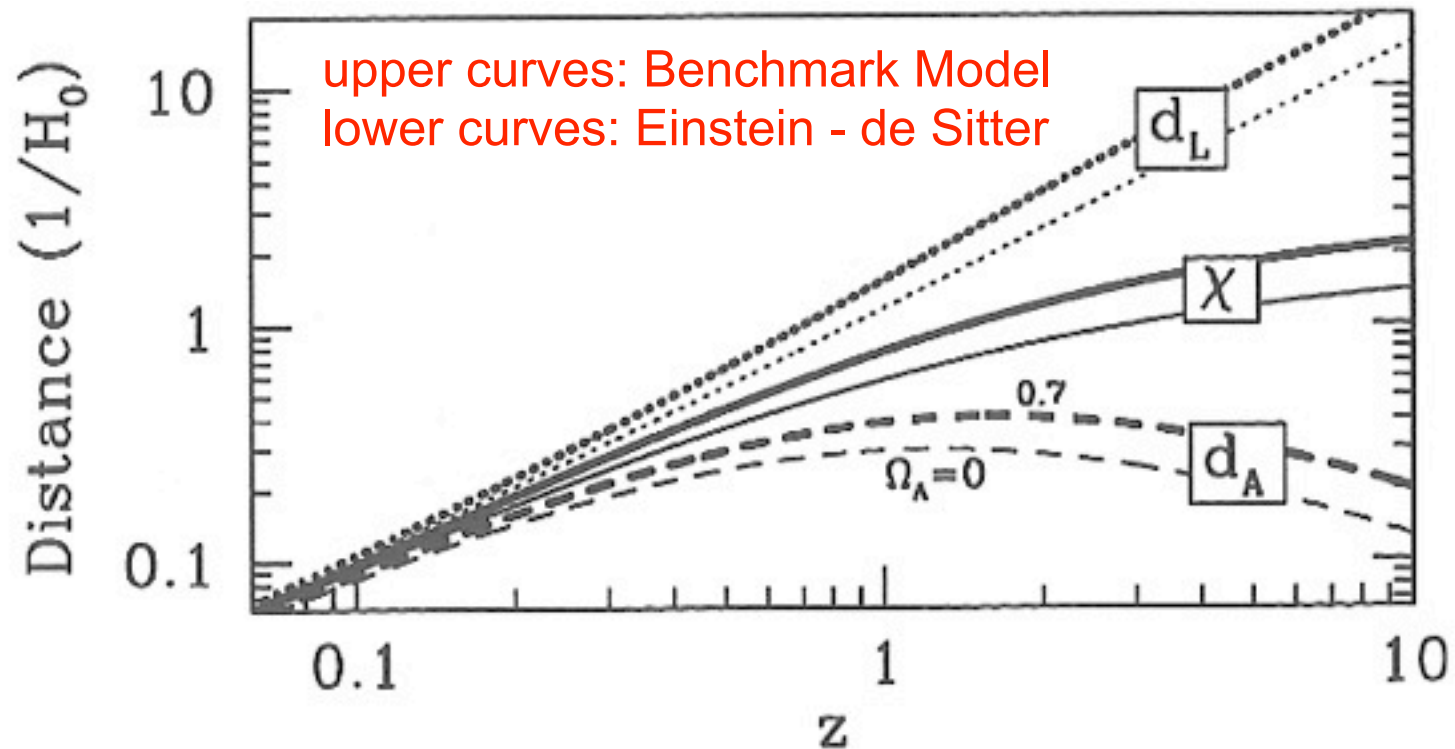


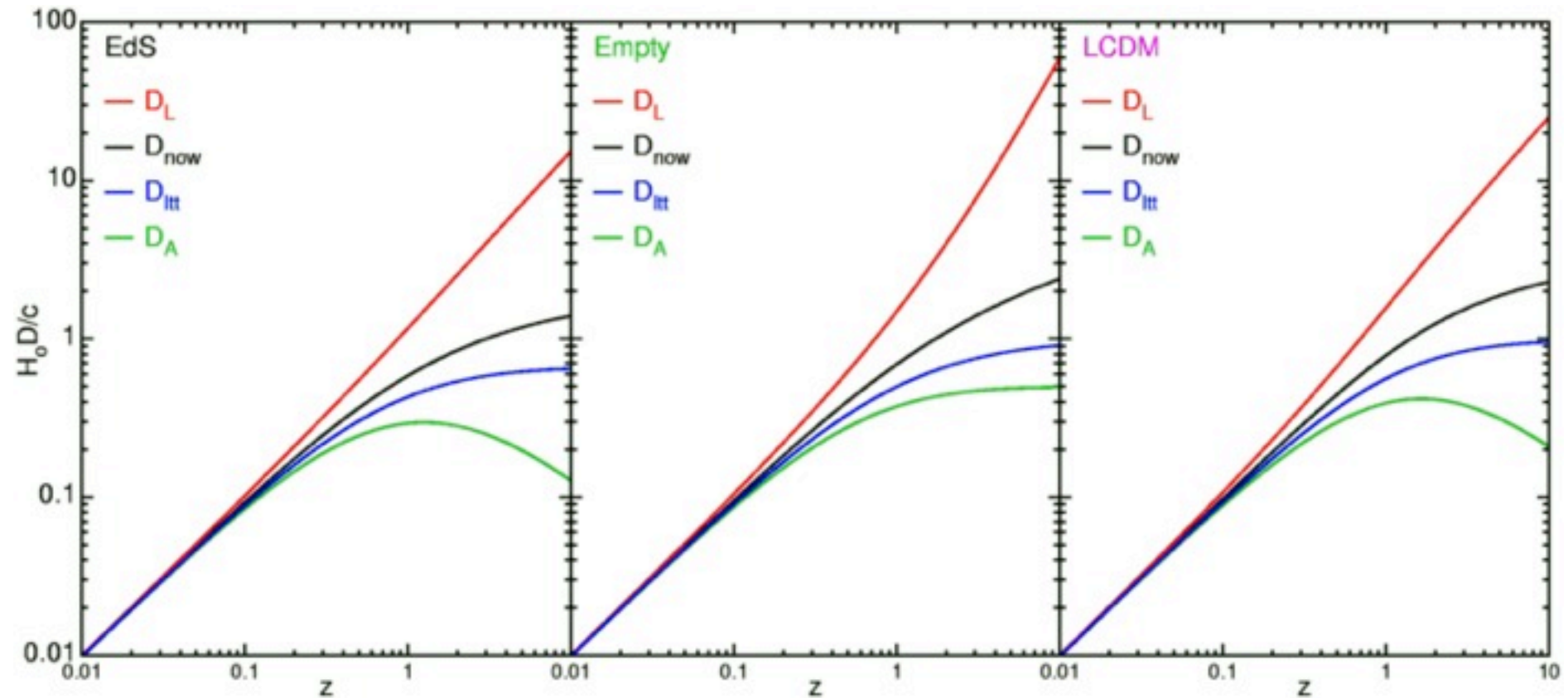
Figure 2.3. Three distance measures in a flat expanding universe. From top to bottom, the luminosity distance, the comoving distance, and the angular diameter distance. The pair of lines in each case is for a flat universe with matter only (light curves) and 70% cosmological constant Λ (heavy curves). In a Λ -dominated universe, distances out to fixed redshift are larger than in a matter-dominated universe.

Scott Dodelson, *Modern Cosmology* (Academic Press, 2003)

Distances in the Expanding Universe

D_{now} = proper distance, D_L = luminosity distance,

D_A = angular diameter distance, $D_{\text{ltt}} = c(t_0 - t_z)$



http://www.astro.ucla.edu/~wright/cosmo_02.htm#DH

Distances in the Expanding Universe: Ned Wright's Javascript Calculator

Enter values, hit a button

H_o
 Ω_M
 z

 Ω_{vac}

Open sets $\Omega_{vac} = 0$ giving an open Universe [if you entered $\Omega_M < 1$]

Flat sets $\Omega_{vac} = 1 - \Omega_M$ giving a flat Universe.

General uses the Ω_{vac} that you entered.

For $H_o = 70$, $\Omega_M = 0.300$, $\Omega_{vac} = 0.700$, $z = 0.830$

- It is now 13.462 Gyr since the Big Bang.
- The age at redshift z was 6.489 Gyr.
- The light travel time was 6.974 Gyr.
- The comoving radial distance, which goes into Hubble's law, is 2868.9 Mpc or 9.357 Gly.
- The comoving volume within redshift z is 98.906 Gpc³.
- The angular size distance D_A is 1567.7 Mpc or 5.1131 Gly.
- This gives a scale of 7.600 kpc/".
- The luminosity distance D_L is 5250.0 Mpc or 17.123 Gly.

$$\begin{aligned} H_o D_L(z=0.83) \\ = 17.123 / 13.97 \\ = 1.23 \end{aligned}$$

1 Gly = 1,000,000,000 light years or 9.461×10^{26} cm.

1 Gyr = 1,000,000,000 years.

1 Mpc = 1,000,000 parsecs = 3.08568×10^{24} cm, or 3,261,566 light years.

[Tutorial: Part 1](#) | [Part 2](#) | [Part 3](#) | [Part 4](#)
[FAQ](#) | [Age](#) | [Distances](#) | [Bibliography](#) | [Relativity](#)

[Ned Wright's home page](#)

© 1999-2003 [Edward L. Wright](#). Last modified on 08/13/2003 11:58:51

<http://www.astro.ucla.edu/~wright/CosmoCalc.html>